The Design of Sluiced Settling Basins:

A numerical modelling approach

Edmund Atkinson
Overseas Development Unit

OD 124
June 1992

HR Wallingford

Address: **HR Wallingford Limited,** Howbery Park, Wallingford, Oxfordshire OX10 8BA, UK
Telephone: 0491 35381 International + 44 491 35381 Telex: 848552 HRSWAL G
Facsimile: 0491 32233 International + 44 491 32233 Registered in England No. 1622174

Abstract

Settling basins can be used to prevent excessively large sediment quantities from entering irrigation canals; they work by trapping sediment in slowly moving flow produced by an enlarged canal section.

The report presents two numerical models which can be used in the design of these structures. One model predicts conditions as a basin fills with sediment: deposition patterns and, more importantly, the sediment quantities passing through the basin are predicted. A second model predicts the sluicing process; in particular it predicts the time required for a basin to be flushed empty using a low level outlet at its downstream end. The models and the assumptions which underly them are described in detail, and model predictions are compared against field measurements from three sites. The models give accurate predictions and are a significant improvement on existing design methods, in both the scope and accuracy of predictions.

Aspects of basin design for which the models do not give guidance include determining the optimum width for a basin, the design of the basin entry and outlet, and the escape channel design. Each aspect is discussed and design methods are presented.

Contents

Contents (Continued)

Tables

Figures

Figures (Continued)

Symbols

a_t	Bed layer thickness	(m)
A_n	A non dimensional number related to adaption length	
A_r	Area ratio of basin entry	
C	Sediment concentration by weight at height y	
C_{aj}	Sediment concentration at top of bed layer for size fraction j	
C_{ej}	Equilibrium sediment concentration at height y for size fraction j	
D_j	Representative grain diameter for sediment size fraction j	(mm)
E	Expansion rate of basin sides at entry	
E_l	Limiting expansion rate	
f	Friction factor defined as $\bar{u}/u_*$	
g	Acceleration due to gravity	(m/s^2)
h	Depth of flow	(m)
h_o	Initial depth in a reach of a basin with a sloping bed, or depth at upstream end of basin as a whole	(m)
h_u	Depth in channel upstream of basin	(m)
h_b	Depth at outlet from expansion at basin entry	(m)
k	A constant of proportionality in equation (21) relating concentration of a size fraction to its size	(units : $m^{2.18}$)
k_s	Bed roughness	(m)
k'	A constant used in equation (25) to relate the proportions of material in transport to those in the bed	(units : $m^{-2.18}$)
p_{bj}	Proportion by weight of the bed material at a particular location consisting of size fraction j	
p_{tj}	Proportion of weight of the material in transport at a particular location consisting of size fraction j	
Q	Design discharge through basin during normal operation	(m^3/s)
Q_s	Design discharge for sluicing	(m^3/s)
q	Flow per m width in a basin	(m^2/s)
R_f	Ratio of retarding friction force to momentum at basin entry	
S	Friction slope of channel	
S_b	Bed slope in a basin	
S_{be}	Bed slope of an entry section to a basin	
S_{gs}	Specific gravity for silt	
u	Velocity at height y	(m/s)
u_c	Centreline velocity at end of basin entry	(m/s)
$\bar{u}$	Mean velocity	(m/s)
u_*	Shear velocity = $(gSh)^{1/2}$	(m/s)
u_{*f}	Shear velocity as predicted by an alluvial friction calculation	(m/s)
V_s	Settling velocity for a representative sand size in transport	(m/s)
V_{sj}	Settling velocity of sediment of size fraction j	(m/s)
W_b	Basin width immediately downstream of inlet	(m)
W_{dmax}	Maximum allowable width for desposition phase of basin operation	(m)
W_{smax}	Maximum allowable width for basin sluicing	(m)
W_u	Width of channel upstream of basin	(m)
x	Distance co-ordinate along a basin of sluice channel	(m)
x_a	Adaption length for the decay of extra turbulence at a basin inlet (deposition model) or for sand concentration within a sub-reach (sluicing model)	(m)
X	Total concentration at a location in the basin for all sand size fractions	

Symbols (Continued)

X_{in}	Sand concentration entering a sub-reach in the sluicing model	
X_{out}	Sand concentration leaving a sub-reach in the sluicing model	
X_T	Total transporting capacity	
X_{Tj}	Sediment transporting capacity for size fraction j, a concentration by weight	
X_{Tsj}	Transporting capacity for silt size fraction j, a concentration by weight	
$X_{Tsj\ vol}$	Transporting capacity for silt size fraction j, a concentration by volume	
y	Height above bed	(m)
α	Non-dimensional height above bed = y/h	
ϵ_x	Sediment diffusion coefficient in x direction	(m^2/s)
ϵ_y	Sediment diffusion coefficient in y direction	(m^2/s)
ϵ_s	Sediment diffusion coefficient	(m^2/s)
ν_t	Laminar viscosity	(m^2/s)
ν_{tf}	Turbulent viscosity caused by bed roughness	(m^2/s)
ν_t	Turbulent viscosity at distance x from basin inlet (depth averaged)	(m^2/s)
ν_{to}	Turbulent viscosity caused by the inlet condistion of a basin	(m^2/s)
ν_{te}	Additional kinematic turbulent viscosity dur to flow expansion	(m^2/s)
ν_{tl}	Extra turbulence at inlet to a settling basin reach above the turbulence produced by roughness and expansion	(m^2/s)
ρ	Water desity	(kg/m^3)
τ_o	Bed shear ($=u_*^2 \rho$)	(N/m^2)

1 Introduction

Sluiced settling basins are usually located at the headworks of an irrigation canal system. Their purpose is to trap the excessive quantities of river sediment which can be brought into an irrigation system, and so prevent sediment from settling in the canal network. A typical settling basin consists of a length of canal with a greatly enlarged cross-section, this causes the flow velocity to be reduced and so sediment is deposited. If there is a sufficient difference in level between the basin's water surface and a suitable discharging point, then the basin can be gravity sluiced when it has been filled with sediment. Sluicing interrupts supplies for irrigation, unless a twin basin design is used, but the interruption is usually short and infrequent.

An example of a design for a sluiced settling basin is shown in Figure 1, the basin at the Karangtalun intake in Central Java. A difference in level between the basin's water surface and the discharging point in the river is produced both by the weir across the river and by a large difference between the river slope and the basin's water surface slope. The difference in level allows effective sluicing of the basin.

A similar means of controlling sediment is to allow it to settle in a sluice channel or "sluicing pocket" located just upstream of the intake gates to a canal. The channel is separated from the main river channel by means of a bund or divide wall and is sluiced by opening sluice gates at its downstream end. The system is often called still pond regulation, an example is shown in Figure 2. Still pond regulation forms part of the sediment control effect at large barrages, where the first few gates of the barrage are separated by a divide wall and so become sluice gates for a sluicing pocket. Operation is the same as for sluiced settling basins: occasionally the canal is closed and the sluice gates opened.

When designing a settling basin or sluice channel an engineer needs to be able to predict its performance, so that he can have confidence that it will be able to prevent canal sedimentation. Prediction can also be used to optimise the design. Three key predictions are required:

(i) the sediment concentration and grain sizes passing into the canal downstream from the basin;
(ii) the frequency of sluicing required; and
(iii) the time required to flush the basin.

Empirical prediction methods for settling basins have been available since the publication of Hazen's equation (Hazen, 1904). Vetter's equation (Vetter, 1940) and Camp's curves (Camp, 1946) are probably the most widely used methods today; Camp's method is recommended in a recently published design guide for sediment control at intakes (Avery, 1989). A method published since the design guide is that due to Garde et al (1990), which is based on extensive laboratory data.

These methods cover only the settling phase of a basin's operation and are restricted in their applicability, they do not include the following factors:

(i) the sediment transporting capacity of the flow in a settling reach (it is assumed to be zero);
(ii) the change in conditions as a settling basin fills with sediment;
(iii) the effect of variation in flow depth down a basin; and
(iv) the additional turbulence produced by the inlet condition to a basin.

These drawbacks mean that existing empirical methods can predict only the trapping efficiency of an idealised basin, they cannot be used to predict the required frequency or duration of sluicing.

This report presents a new approach, the use of numerical modelling to simulate the flow in settling basins and hence make the performance predictions required to evolve a design.

Two categories of numerical model have been developed in recent years which could be applied to sedimentation in a settling basin on an irrigation canal. Firstly there are numerical models which predict the flow and sediment concentrations in sedimentation tanks at sewage or water treatment works, for example the model presented by Adams and Rodi (1990). These models include the effect of turbulence produced by inlet conditions but do not include the sediment transporting capacity of the flow or changes in behaviour as a tank fills (such effects are not important in sedimentation tanks where flow velocities do not exceed a few centimetres per second and tanks are not designed to fill with deposited material).

A second category of numerical model which might be applied to sedimentation in a settling basin is the non-uniform suspended sediment transport model, examples include the models described in Bechteler and Schrimf (1983) and Kerssens et al (1979). The application of a model similar to the Kerssens model is described in this report, however extensive development of the method has been required to enable the turbulence produced by sources other than bed friction to be included, to include simulation of silt, to predict the bed material grain sizes and to enable the model to run sufficiently rapidly even when many sediment size fractions are taken.

This report presents the model which simulates sediment deposition in a basin together with a second model which simulates sluicing. The models and their underlying assumptions are described in the next chapter, while Chapter 3 presents their verification using field data. Both models are width averaged so they cannot be used to design the inlet to a settling basin, or to determine the maximum allowable width. Therefore these aspects of settling basin design are discussed in Chapter 4.

Conclusions of the study are given in Chapter 5.

2 Description of models

Initial work on these models is described in an earlier report (Atkinson, 1986a), they have been developed considerably since that publication.

2.1 Sediment deposition model

2.1.1 Overall structure of model

The model for simulating sediment deposition in a settling basin or sluice channel is described in outline in a flow chart, Figure 3, the overall structure is also described below.

The basin is split into short sub-reaches and the filling period into short time steps, within each time step steady conditions are assumed. Calculations for an individual time step begin with a backwater calculation to obtain the water levels in the basin from a known water level at the downstream end. The discharge and bed levels at the start of the time step are required for this computation, while the roughness of the sediment deposits is predicted using an alluvial friction predictor.

Turbulence intensities in the basin are then calculated, turbulence is generated by three sources: the gradually expanding flow in a basin, friction at the bed and inlet conditions.

Sand sized sediment entering the basin is split into ten equal size fractions, the concentrations of each fraction are then traced down the basin. Concentrations are calculated at ten heights above the bed at each section in the basin, the concentration change between one section and the next downstream (ie. within a sub-reach) is computed from a turbulent diffusion equation. The input to the computation includes turbulent viscosity, the settling velocity and the concentration at the bed. The sediment concentration at the bed is itself calculated, for each size fraction, from grain size, the proportion of the bed material which consists of that fraction and the hydraulic conditions in that sub-reach of the basin.

Once the concentrations and hence the transport rates of each of the sediment size fractions are known the rate of sediment deposition in each sub-reach of the basin can be calculated using the concept of continuity. The proportions of each fraction within the total rate of sediment deposition are used to derive the size grading of the depositing material in each basin sub-reach. The total rate of deposition, together with a value for the density of settled sediment, yields a value for the bed level rise at each sub-reach. The new bed levels and the bed material size gradings are used as input to the computations for the next time step.

The computation requires an iteration at the start of the filling process because the sediment size grading of the first deposits is both required for the calculation and predicted by it. Thereafter predictions from one time step are used as input to the subsequent time step.

At each time step the concentrations of each fraction leaving the basin are used to determine both the total concentration leaving the basin and its size grading. These are the key predictions of the model, a designer can use them to decide if the concentrations and sediment sizes leaving a basin are sufficiently small, and if they remain small for a sufficient time. If the basin's performance is not acceptable then a larger basin can be tested.

This section has presented the overall structure of the model, certain more detailed aspects are now discussed.

2.1.2 De-coupling of the water and sediment computations

Within each time step steady conditions are assumed and a single set of bed levels are taken, these assumptions de-couple the steady state backwater calculation from the calculations of sediment transport. They are justified because the propagation speed of water surface disturbances, and hence adjustment to steady state, is much larger than the propagation rate of the bed accretion. This approach has been commonly used in one-dimensional river models, where the application involves much greater variations in water surface elevations than is found in settling basins. A more detailed account of its justification is given in Bettess and White (1979).

2.1.3 Calculation of turbulence

Turbulence is derived from three separate sources in a settling reach: the roughness of the bed features, the gradual flow expansion (caused by the depth increasing in the downstream direction) and the inlet conditions. If the turbulence level was calculated only from the friction slope (ie. the slope obtained from the backwater calculation), then only the first of these sources would be accounted for. To simulate the other sources of turbulence a turbulence model was used. (Turbulence models are semi-empirical equations which describe the generation and decay of turbulence within a fluid and at its flow boundaries). The computer coding required is relatively complex so an approach using a commercially available computer package for flow simulation, which incorporates turbulence models, has been adopted.

Simulations are made on a grid of computational cells and an iterative technique is used to obtain a solution to the Navier-Stokes equations (the set of equations which describe fluid flow). A range of turbulence models are available in the package, the well established k-ϵ model was selected due to its wide usage and successful application to flow in rivers (Rodi, 1984).

The computer package was used to simulate the flow in settling basins and so to produce a set of simple equations which predict the effect that expansions and inlet conditions have on turbulence.

A typical set of results is shown in Figure 4, which gives a plot of kinematic turbulent viscosity against distance from the inlet in an idealised basin of uniform width with a continuously sloping bed. Kinematic turbulent viscosity is chosen to represent turbulence as it is directly related to the mixing effect of turbulence and hence its effect on retarding sediment deposition. There was a small variation of kinematic viscosity with height above the bed, but Figure 4 shows depth averaged values. The inlet condition for the simulation shown in Figure 4 was a smooth entry: a long channel with the same depth and roughness as at the upstream end of the basin. The graph also shows the turbulent kinematic viscosity in the basin which is due to the bed friction alone, it was obtained by undertaking a separate set of simulations for uniform channels. For example, at 200m from the basin inlet the depth is 3m for the conditions given in Figure 4, and so the turbulence due to friction was calculated from a simulation of a uniform 3m deep channel. The graphs show that there was a roughly constant additional turbulence caused by the sloping bed in the basin once a transition effect had decayed. This observation was

also found for the simulations with other conditions. It was assumed, therefore, that turbulence caused by the inlet conditions and the turbulence caused by the sloping bed could be added to that caused by friction at the bed.

The simulations also showed that the behaviour could be approximated to the exponential decay of an initial turbulence level, caused by the inlet conditions, to a constant value of additional turbulence caused by the sloping bed.

Dimensional analysis was used to determine an expected form for the relationship between a basin's bed slope and the stable level of additional turbulence which it causes. This additional kinematic turbulent viscosity, ν_{te}, is expected to be a function of:

initial depth, h_o,
laminar viscosity, ν_l,
mean velocity, $\bar{u}$,
bed roughness, k_s,
bed slope, S_b, and
fluid density, ρ.

There are six independent variables with three dimensions so we can expect ν_{te} to depend on three non-dimensional numbers:

$$\frac{\nu_{te}}{h\,\bar{u}} = F\left[\frac{h_o\,\bar{u}}{\nu_l}, \frac{k_s}{h_o}, S_b\right] \qquad (1)$$

The first number is a Reynolds number, a typical value in a field scale settling basin would be around 10^6, well above the values at which a Reynolds number will have a significant effect. The second number was also found to produce an insignificant affect on additional turbulence, its principal effect was on the turbulence produced by the rough bed. A relation for ν_{te} was found by fitting a curve through values of ν_{te} and S_b predicted by the flow simulation computer package:

$$\nu_{te} = 0.0986\, S_b^{0.84}\, q \qquad \text{if } S_b < 0.06 \qquad (2)$$

and

$$\nu_{te} = q\,(0.00148 + 0.13\, S_b) \qquad \text{if } S_b > 0.06 \qquad (3)$$

where $q = \bar{u}\,h$

A similar approach was used to derive a relation for adaption length, x_a, for use in the exponential decay function:

$$x_a = \frac{A_n\, h_o}{1.6\,(2 - S_b\, A_n)} \qquad (4)$$

$$\text{where} \quad A_n = 7.6 + \left(20.2 - 5.2 \ln\left(\frac{k_s}{h_o}\right)\right) e^{-14.9\, S_b} \qquad (5)$$

The turbulent viscosity in a basin, ν_t, is thus calculated:

$$\nu_t = \nu_{tf} + \nu_{ti}\, e^{-x/x_a} + \nu_{te} \qquad (6)$$

where ν_{tf} = turbulence produced by bed friction
ν_{ti} = initial extra turbulence at the
x = distance from inlet, and
x_a = adaption length.

The ν terms in equation (6) are all depth averaged values of turbulent viscosity.

The turbulent viscosity due to bed friction, ν_{tf}, must be determined. A value for turbulent mixing of sediment ("eddy diffusivity" or ϵ_s) can be obtained using the Lane and Kalinske (1942) formula which assumes uniform flow:

$$\epsilon_{sf} = \frac{h\, u_*}{15} \qquad (7)$$

where ϵ_{sf} is the value of ϵ_s when only bed friction is producing turbulence, and u_* is shear velocity.

If the turbulent Schmidt number, ν_t/ϵ_s, is assumed to be unity then eddy diffusivity is equivalent to kinematic turbulent viscosity. Equation (6) can then be re-written:

$$\epsilon_s = \frac{h\, u_*}{15} + \nu_{ti}\, e^{-x/x_a} + \nu_{te} \qquad (8)$$

The shear velocity is obtained from alluvial friction calculations.

A settling basin during its filling process rarely has the simple geometry of an empty basin with a continuous bed slope. The method is applied therefore by imagining that the basin is made up from numerous small basins, themselves each having a simple geometry. The value for turbulent viscosity at the end of one small basin is the inlet value for the next basin downstream. These small basins within the overall basin correspond to the sub-reaches into which a settling basin is divided (Section 2.1.1 above).

The value for turbulent viscosity at the upstream end of a settling basin, ν_{to}, is strongly dependent on inlet geometry, and so further flow simulations were performed with the computer package to derive functions for ν_{to}. The following approximate relationships can be used if the basin entry geometry is a simple expansion from a channel. If the inlet expansion has either a rising bed or no bed slope at all:

$$\nu_{to} = 0.01\, \frac{Q}{W_b} \qquad (9)$$

where Q is the basin discharge, and
W_b is the basin's width at its upstream end.

If there is a downward bed slope:

$$\nu_{to} = 0.01 \frac{Q}{W_b} + (0.0015 + 0.13 S_{be}) \frac{Q}{W_u} \qquad (10)$$

where S_{be} is the downslope of the expansion at the basin entry, and
W_u is the width of channel upstream of the basin.

The deviation of equations (9) and (10) is given in Section 4.1. They apply only to entry sections which comply with the design recommendations given in that section.

Basin entry designs with more complex geometries must be simulated individually with a flow simulation package, to obtain a value for ν_{to}.

2.1.4 Modelling the effect of turbulence on sediment concentrations

Sediment settling under the influence of gravity is offset by the mixing produced by turbulence in the flow. This process is described by the following basic equation, which is given in Dobbins (1944):

$$u \frac{\partial C_j}{\partial x} = \epsilon_y \frac{\partial^2 C_j}{\partial y^2} + \left(V_{sj} + \frac{\partial \epsilon_y}{\partial y} \right) \frac{\partial C_j}{\partial y} + \epsilon_x \frac{\partial^2 C_j}{\partial x^2} \qquad (11)$$

where u = flow velocity at height y above the bed (m/s)
y = height above bed (m)
C_j = sediment concentration at height y above bed for size fraction j
x = distance co-ordinate along channel (m)
ϵ_y = sediment diffusion coefficient in y direction (m^2/s)
ϵ_x = sediment diffusion coefficient in x direction (m^2/s), and
V_{sj} = settling velocity of sediment for the sediment size fraction j (m/s). It is calculated in the model using the Gibbs et al (1971) formula.

It is assumed in Equation (11) that the velocities and concentrations are constant across the width of the channel, that the flow is steady and that the concentrations in one size fraction do not affect other size fractions.

It can further be assumed that the diffusion in the x direction is insignificant (Dobbins, 1944). The diffusion coefficient ϵ_y is ϵ_s of Section 2.1.3, an expression for ϵ_s was given by Equation (8):

$$\epsilon_s = \frac{h u_*}{15} + \nu_{ti} e^{-x/x_a} + \nu_{to} \qquad (12)$$

Implicit in the use of equation (12) is the assumption that a depth averaged value of ϵ_s can be taken. The simulations using PHOENICS reported in the previous section did show a small variation of turbulent viscosity with height above the bed, however, the errors introduced by using a depth averaged diffusivity are expected to be small. Kerssens et al (1979) tested alternative formulations for ϵ_s in a numerical model based on equation (11), they found only small differences in results when the ϵ_s formulation was changed from a depth averaged one to a formulation including variations with height.

Equation (11) now becomes:

$$u \frac{\partial C_j}{\partial x} = \epsilon_s \frac{\partial^2 C_j}{\partial y^2} + V_{sj} \frac{\partial C_j}{\partial y} \qquad (13)$$

The solution of this equation is used to obtain sediment concentrations at ten heights above the bed within each sub-reach of a basin. Figure 5 shows the problem to be solved: the input concentration profile to a sub-reach is known for a sediment size fraction, its transporting capacity can be derived using a sediment transport predictor (see Section 2.1.5 below), and from these the concentration profile leaving the sub-reach is required. The sub-reaches in the computational scheme are short, so hydraulic conditions can be assumed to be uniform within each sub-reach.

The bed layer is assumed to have a constant thickness, a_t, which is taken as 5% of the flow depth; within the bed layer a uniform concentration is assumed. Other values for a_t could be chosen, but the effect on the predictions of the model would be small (Kerssens et al, 1979). Concentrations are to be predicted using Equation (13) from the top of the bed layer to the water surface.

The water surface boundary condition is simply that sediment cannot pass through the surface:

$$V_{sj} C_j + \epsilon_s \frac{\partial C_j}{\partial y} = 0 \qquad \text{at } y = h \qquad (14)$$

At the bed boundary we assume that the suspended sediment concentrations immediately above the bed layer do not directly affect conditions within the bed layer. The bed boundary condition can then be taken as a fixed entrainment rate from the bed layer. The entrainment rate is derived from the sediment concentration in the bed layer, C_{aj}:

$$\frac{\partial C_j}{\partial y} = - \frac{V_{sj} C_{aj}}{\epsilon_s} \qquad \text{at } y = a_t \qquad (15)$$

The calculation of C_{aj} for each sediment size fraction is discussed in the next section.

Once the basic equation describing the turbulent diffusion (Equation 13) and the boundary conditions (C_{aj} and Equations 14 and 15) have been determined, then the concentration profile leaving each sub-reach in a basin can be computed from the profile entering the sub-reach.

Unfortunately, the basic equation cannot be solved analytically because the velocity profile is not uniform. The model described by Kerssens et al (1979) used an implicit numerical scheme to solve the equation; this approach involves many small distance steps in the computation and so is prohibitively time consuming, especially when more than one sediment size fraction is being modelled. Details of the method are set out in Bechteler and Schrimpf (1983).

The approach used for the model described in this report was to assume initially that the velocity profile was uniform and then, if necessary, to

compensate for the errors that this assumption introduced.

Predictions using a uniform velocity profile were compared with those using a logarithmic profile:

$$u = \bar{u} + 2.5\, u_* (\ln \alpha + 1) \qquad (16)$$

where $\alpha = y/h$
and von Karman's constant has been taken as 0.4.

The effect of the shape of the velocity profile was assessed using a model which was similar to the model described by Kerssens et al (1979). Results are presented in Figure 6 which shows concentrations predicted for both shapes of velocity profile. The conditions were:

$\bar{u}/u_*$ = 10 (a low value, so that the difference in velocity profiles would be large)
h = 1.0m
a_t = 0.05m
V_{sj}/u_* = 0.1.

Initial values for C were set at zero; this produced a sudden change in sediment concentrations and so maximised the effect of a difference between the velocity profiles.

The maximum error in mean concentration produced by these conditions was only about 2% of the transporting capacity. Therefore, the errors introduced by assuming a uniform velocity profile are small, and the assumption can be taken without the need for error compensation.

The analytical solution of Equation (13) was achieved using an approach which employed Fourier analysis. An example of an analytical solution to the equation is given in Dobbins (1944), where a different bed boundary condition is used.

2.1.5 Determining the sediment concentration at the bed boundary

The bed boundary condition, Equation (15), included a value for sediment concentration in the bed layer, C_{aj}. A value is required for each sub-reach of the basin and for each sediment size fraction.

It has been assumed that the bed concentration, C_{aj}, is not affected by the concentrations in the flow above the bed, and so C_{aj} adapts immediately to changes in hydraulic conditions down a basin. It follows that C_{aj} is equal to the bed concentration in a long channel with the same hydraulic conditions, that is a channel which has reached equilibrium and so its sediment load is equal to transporting capacity. Therefore, the transporting capacity for a size fraction, X_{Tj}, and the integral of an equilibrium concentration profile can be equated to derive an expression for C_{aj}:

$$X_{Tj}\, h = \int_0^h C_{sj}\, dy \qquad (17)$$

where C_{ej} is the equilibrium concentration profile

$$C_{ej} = C_{aj} e^{-(y - a_1) V_{sj}/\epsilon_s} \qquad \text{for } y \geq a_1 \tag{18}$$

and C_{ej} is equal to C_{aj} if $y \leq a_1$

Equation (18) is derived from the special case of Equation (13) when the channel is in equilibrium:

$$\epsilon_s \frac{\partial C_j}{\partial y} + V_{sj} C_j = 0 \tag{19}$$

The bed concentration, C_{aj}, can therefore be obtained from X_{Tj}, V_{sj}, ϵ_s and a_1.

The sediment transporting capacity, X_{Tj}, is required for each size fraction and at each location in the basin. The total sediment transporting capacity, for all size fractions, X_T, can be predicted using a method such as the Engelund and Hansen (1967) formula or the Ackers and White (1973) formulae. These methods require the following input: depth, mean velocity, width, shear velocity (or friction slope) and bed material grain sizes.

The model uses an enhanced shear velocity as an input to the sediment transport calculation so that the effect of additional turbulence on sediment transport can be simulated. A relationship between the eddy diffusivity obtained from Equation (8) and the enhanced shear velocity can be derived from the Lane and Kalinske formula, (Equation 7):

$$\text{enhanced shear velocity} = \frac{15\ \epsilon_s}{h} \tag{20}$$

The transporting capacity for an individual size fraction must be predicted from the total sediment transporting capacity. It is a function of the representative sediment grain diameter for the fraction, D_j, and the proportion of the bed material which consists of that size, p_{bj}. (The sum of the p_{bj} values for all fractions is unity.)

The following empirical equation is used:

$$X_{Tj} = k\, p_{bj}\, D_j^{-2.18} \tag{21}$$

where the constant, k, is set so that the sum of the X_{Tj} values equal the total transporting capacity, X_T:

$$k = \frac{X_T}{\Sigma\, p_{bj}\, D_j^{-2.18}} \tag{22}$$

Equation (21) was derived by assuming that the sediment sizes and the flow conditions independently affect the sediment transport rate of an individual size fraction (in the same way as is implied by the Engelund and Hansen sediment transport prediction equation). The form of the function of D_j in Equation (21), and the value of its exponent, were obtained by comparing

measured sediment sizes in transport with measured bed material size gradings at five field sites. The work is reported in the Appendix of Atkinson (1987).

2.1.6 Modelling silt deposition

Most settling basins and sluice channels designed for irrigation canal systems are intended to trap only sand and coarser sediments, because it is assumed that silt and clay can be transported through the canal network. However, silt deposition can be a significant problem in the smaller canals of an irrigation system and, more generally, sand storage in a settling basin can be greatly reduced by silt deposition. These effects necessitate the inclusion of silt deposition in the simulations performed by the settling basin model.

Silt transport and deposition cannot be modelled merely by specifying silt sized sediment fractions in the model; there are three reasons. Firstly, the sediment transport equations used by the model do not apply to silt sized sediment. Secondly, silt tends to settle with a much lower bed material density than sand, so a single density cannot be specified if a mixture of silt and sand is entering a basin. Thirdly, silt is cohesive so when it has settled it then requires a larger shear to cause it to be re-suspended. Therefore the concepts of a continuous interchange between bed material and suspended material cannot be used for silt, indeed large silt concentrations can be transported when no silt is present in the bed material.

These problems are overcome by considering the silt and sand separately. A sediment transport relationship for silt sized sediment is available, Westrich and Jurashek (1985), the method gives predictions of transporting capacity which are independent of bed material composition.

$$X_{Tsj\ vol} = \frac{0.0018\,\tau_o\,\bar{u}}{(S_{gs} - 1)\,\rho\,g\,h\,V_{sj}} \qquad (23)$$

where $X_{Tsj\ vol}$ is the transporting capacity of a silt fraction in terms of a concentration by volume (not by weight as is used elsewhere in this report),

τ_o is the bed shear, $\tau_o = u_*^2 \rho$,

ρ is water density,

S_{gs} is the specific gravity of silt, and

V_{sj} is the silt fraction's settling velocity.

$X_{Tsj\ vol}$ is converted to a concentration by weight using the following relationship:

$$X_{Tsj} = \frac{X_{Tsj\ vol}\,S_{gs}}{1 - X_{Tsj\ vol} + X_{Tsj\ vol}\,S_{gs}} \qquad (24)$$

Equation (23) was developed using laboratory tests with settling velocities ranging from about 0.4mm/s to about 9mm/s.

The laboratory tests were conducted with sediments having a single settling velocity fraction, and so an assumption is required to apply Equation (23) to sediment consisting of a range of settling velocity fractions. It is common to assume that the quantity of each sediment fraction in suspension is

independent of the other fractions, this has been assumed for the sand simulations. The link between sand fractions is determined from their proportions in the bed material, Equation (21). However this cannot be used for Equation (23) because bed material composition does not affect concentrations of silt and clay.

Some link between fractions is required, otherwise increasing the number of fractions selected would artificially cause the predicted transporting capacity to increase. We overcome the difficulty by assuming that sediment sizes smaller than 63 microns are not affected by larger sizes, and that silt or clay size fractions can be considered to be independent when their settling velocity range covers a twofold change in settling velocity. We should expect the constant in Equation (23) to change as the chosen range of settling velocity within a silt fraction is changed, so the equation needs re-calibrating for our assumption. The constant was found to be doubled, to 0.0036, when the method was compared with data from the canals of the Gezira irrigation scheme in Sudan, see Section 3.4. The data covered a discharge range of $0.2m^3/s$ to $8m^3/s$ and the sediment composition ranged from clays to coarse silts.

In other respects the silt fractions are simulated like the sand fractions. Total rise in bed level is calculated for all sand fractions and for all silt fractions separately, because different bed material densities apply to sand and silt, and then they are combined to obtain total bed level rise for each section of the basin.

Any effects of silt flocculation, and hence changes in silt settling velocity, are ignored because detention times in typical basins for irrigation systems are short relative to the time period in natural flocculation processes.

2.1.7 Output for sluicing simulation

The predictions of the sediment deposition model not only provide estimates of the concentrations and sediment sizes passing through a basin, they also provide part of the input to the simulation of sluicing. The sluicing model requires initial bed levels and bed composition, in terms of sediment sizes and densities, in order to predict sluicing performance. This information is stored by the deposition model as the simulation proceeds, it keeps an inventory of the bed material sizes and density at each height above the bed for each section in the basin. Only sand sizes are stored because the sluicing model simulates only sand movement; it is assumed that any silt in the exposed bed material is sluiced instantly and so only the sand transport controls sluicing rates. Likewise bed material density relates only to sand; it is defined as weight of sand per unit volume of deposited material.

2.1.8 Sediment re-working during deposition

If, after a period of deposition, the discharge entering a basin increases or the concentration reduces then re-working can be expected. This process is not simulated in the model because it would require complex programming involving the effect of different rates of erosion for each size fraction and hence armouring of the deposited material. It is assumed that once silt or sand has settled in a basin it will not be eroded again until the basin is sluiced. The approximation does not significantly effect the overall utility of the model because sediment re-working only occurs near the upstream end of a basin,

while it is conditions at the downstream end which directly affect the sediment concentrations and sizes leaving a basin.

A prediction of bed material size grading is nevertheless required for those reaches where no sand deposition is occurring and hence the method of prediction described in Section 2.1.5 cannot be used. For these circumstances the bed material grading is predicted directly from the grading of the material in transport; the inverse of Equation (21) is used:

$$p_{bj} = \frac{k' p_{tj}}{D_j^{-2.18}} \qquad (25)$$

where p_{tj} is the proportion of size fraction j within the material in transport, and where the constant, k', is now set so that the sum of the p_{bj} values equals unity:

$$k' = \frac{1}{\Sigma p_{tj} D_j^{2.18}} \qquad (26)$$

The threshold between the two methods of bed material prediction is:

If $X \leq 1.1\ X_T$ the method just described is used.

If $X > 1.1\ X_T$ the deposition method described in Section 2.1.5 is used.

X is the total concentration for all sand sized fractions and X_T is the total sand transporting capacity.

This choice of threshold ensures that a bed material prediction is possible even for conditions where some size fractions are depositing and others are eroding within a net deposition of material. There was no noticeable discontinuity in the predictions of bed material grading using this method when the threshold was crossed, so the method was considered satisfactory.

2.2 Sediment sluicing model

2.2.1 Overall structure

The model for simulating sluicing in a settling basin or sluice channel has a similar overall structure to that of the deposition model, it is shown in a flow chart, Figure 7.

The basin is split into sub-reaches and time into time steps. For each time step the water levels, and hence velocities and friction slopes, are calculated; this leads to a calculation of sediment transporting capacity in each sub-reach of the basin. Sand concentrations can then be traced down a basin from the low concentrations entering the basin to high concentrations at the outlet. Changes in concentration from one sub-reach to the next are used to compute changes in bed level for the time step, then the next time step can be taken. The cycle is continued until the basin is empty.

Bed level changes predicted from sediment concentrations may be adjusted, for example if the predicted change implies scour below the concrete bed of a basin, these adjustments are discussed in Section 2.2.6 below.

2.2.2 Silt simulation

Unlike the deposition model, the sluicing model does not simulate silt transport, instead the assumption is taken that silt erodes instantly. This assumption implies that the erosion of a silt and sand mixture is controlled entirely by the predicted rate of sand erosion. (The bed density used in the model is therefore the weight of sand per unit volume of sand and silt). The affect of the assumption is difficult to quantify, it is not clear even whether the presence of silt enhances or impedes sand erosion. The assumption can only be justified within the overall context of a successful comparison between the complete model and field data (Chapter 3).

2.2.3 Single size fraction

A second difference between the deposition and sluicing models is the number of size fractions for sand. The sluicing model uses only a single size fraction because the use of more fractions would not significantly improve the accuracy of the simulations. Many size fractions are only needed where diffusion effects are dominant, and so behaviour of coarser sizes is significantly different from that of finer sizes. For sluicing, it is the sediment transporting capacity of the flow which is the dominant process, and even the most recently developed sediment transport prediction equations use only one size fraction.

Armouring effects (coarser sizes remaining in the deposit while finer sizes are eroded) are not simulated; it is not expected to produce significant inaccuracies because the high bed shear during sluicing exceeds the threshold values for initiation of sediment movement, this applies even for the coarsest sediments being trapped in typical basins.

2.2.4 Diffusion calculation

Diffusion calculations in the sluicing simulation are based on the same equations as for the deposition model. However, the method of application is different. Diffusion is not the dominant process in sluicing, so it can be modelled using the following simplifying equation:

$$X_{out} = X_T - (X_T - X_{in})\, e^{-x/x_a} \qquad (27)$$

where X_{out} is the sand concentration leaving a sub-reach,
X_T is the transporting capacity,
X_{in} is the concentration entering the reach,
x is the length of the reach, and
x_a is an adaption length.

Dimensional analysis shows that the adaption length depends on Reynolds number, friction factor $\bar{u}/u_*$ and the ratio V_s/u_*. Reynolds numbers are high and so their effect can be ignored (see Section 2.1.3). A table of values of non-dimensional adaption length (x_a/h) was prepared using the relevant coding from the deposition model; the table is stored in the sluicing model so x_a can instantly be obtained from the $\bar{u}/u_*$ and V_s/u_* values.

The simulation is greatly speeded by this approximation without a significant loss in accuracy.

2.2.5 *Water level computations*

The calculation of water levels in a basin or sluice channel during sluicing cannot be performed using a backwater calculation alone because the flow is largely supercritical. A combination of frontwater and backwater calculations are required; the method described in Molinas and Yang (1985) has been adopted for the model.

An alluvial channel friction predictor is still used in the calculation; the methods due to Engelund (1966) and Brownlie (1983) were selected because they cover the upper regime conditions associated with high Froude numbers.

2.2.6 *Instability*

The predicted bed level changes are sometimes adjusted before a new set of bed levels are calculated, for example scour to below the concrete bed of a basin is prevented by adjusting predicted bed level changes. However some further adjustment is required due to a basic instability in the process being modelled.

Supercritical flow in a basin causes the downstream water level to have no immediate effect on water levels in most or all of the basin, because only upstream conditions can effect supercritical flow. However, the overall process is controlled by the downstream water level: the lower this level is set the higher the rate of sluicing. These apparently conflicting concepts are reconciled by the effect of hydraulic jumps which cause sudden discontinuities in the pattern of scour and re-deposition in a basin. Hydraulic jumps tend to migrate upstream as the erosion proceeds.

When the process is modelled at a set of discrete points or nodes (each representing a sub-reach) the position of a hydraulic jump rarely coincides exactly with a node, and so difficulties arise. The effect is not complete divergence in the simulation but an unrealistically irregular set of bed levels are produced.

To overcome this difficulty the pattern of deposition downstream from a hydraulic jump is adjusted to smooth out the irregularities caused by the jump when it was located further downstream. In addition predicted erosion at the node immediately upstream of a jump can cause a bed level lower than that just downstream of the jump; this also is prevented. These adjustments have overcome the instability problems without themselves imposing the pattern of scour in a basin during sluicing.

3 Field verification

This chapter presents the field verification of the models described in Chapter 2. Laboratory data has not been used, verification of the models at a field scale is more directly appropriate to design and so carries greater credence with design engineers.

The deposition and sluicing models have each been compared with data from three sediment traps. At the first site the models are verified independently while at the other two sites a combined model is verified: the bed material

densities and size gradings predicted by the deposition model are used as input to the sluicing model.

The deposition model has also been compared with data from an irrigation system where silt depositon in canal headreaches is severe.

3.1 Sluice Channel at the Mae Tang Intake

3.1.1 Description

The Mae Tang canal serves an irrigated area around Chang Mai in the North of Thailand. It was constructed in the 1960's and has a design discharge of 23m^3/s. A plan view of the intake is presented in Figure 2, which shows how a sluice channel has been incorporated upstream from the canal intake gates. The channel is sluiced at approximately monthly intervals during the wet season by closing the canal gates and opening the sluice gates; sluicing typically takes a few hours.

The performance of the intake was monitored from September 1984 to November 1985 in a collaborative study undertaken by the Royal Irrigation Department of Thailand and HR Wallingford. The purpose of the study was to investigate the performance of diversion weirs in rivers carrying high sediment loads, so a detailed monitoring of the performance of the sluice channel itself was not initially undertaken.

However, a detailed set of measurements in the sluice channel was made on 26th September 1985 and another set of measurements was undertaken when the channel was sluiced in November 1986.

The field study is reported in Atkinson (1986b); the report includes a comparison between earlier versions of the prediction models and field data.

3.1.2 Comparison with deposition model

The data used for input to the deposition model are presented in Table 1. Some assumptions had to be made to derive the data given in Table 1, the more important ones are discussed below. Firstly, the upstream boundary of the settling reach was assumed to be unaffected by the swirling flow produced at the bend. However, the swirling flow would tend to keep the sediment in suspension, so the location of the upstream boundary was not taken as the sluice channel entrance. Instead it was assumed to be at about half way around the bend, that is a value of 170m for settling reach length. When a value of 150m was taken, which corresponds to the upstream boundary located at the outlet of the bend, it had little effect on the results: less than a 1ppm change in sediment concentration entering the canal.

The sediment concentration entering the settling reach was obtained from measurements in the river upstream from the abstraction point. An increase of 28% from the river to the settling reach was assumed; this increase accounts for an intake's tendency to abstract proportionately more of the near bed flow, which contains higher sediment concentrations, and less of the faster moving flow near the surface. The value of 28% was derived from numerical modelling using a flow simulation computer code; the code was briefly discussed in Section 2.1.3, but Atkinson (1989) explains this application in more detail. A sensitivity analysis shows that if the 28% increase is ignored

altogether then only a 15% change in sediment concentration entering the canal is obtained.

A final assumption involved the grain sizes entering the sluice channel: they were extrapolated from data collected on other days.

The result of the comparison is shown in Figure 8; it is encouraging. The reduction in sediment concentrations down the sluice channel was predicted using the model and compared with the measured values. The concentration leaving the basin was predicted at 60ppm and measured at 72ppm; these values refer to sand only, no silt measurements were made.

No calibration of the model was used to achieve this result, but results were affected by the choice of alluvial friction and sediment transport prediction method. Four combinations of prediction method were tried, the results are summarised below:

Friction Prediction Method	Sediment Transport Prediction Method	Resulting Prediction of concentration entering canal
White, Paris & Bettess (1979)	Ackers and White (1973)	22ppm
Brownlie (1983)	Brownlie (1981)	41ppm
Engelund (1966)	Engelund and Hansen (1967)	60ppm
van Rijn (1984)	van Rijn (1984)	26ppm

The four pairs of methods were selected because each has been extensively tested against field data. In particular they were in the group of better performing methods in a study undertaken by Meadowcroft (1988), which compared friction and transport prediction methods with a set of field data restricted to the range of conditions found in irrigation canals. It is interesting to note that the Engelund and Hansen sediment transport predictor gives the best results both in the Meadowcroft study and the comparison above.

The Engelund (1966) friction method and Engelund and Hansen (1967) transport method were therefore chosen for subsequent comparisons between the deposition model and field data.

3.1.3 Comparison with sluicing model

The data used for input to the sluicing model are presented in Table 2. The upstream boundary of the sluice channel is now taken at the channel entrance, the bend is not expected to affect the sluicing performance significantly because the flow is faster and shallower and so the swirling effect is much less significant. A 400m long river reach upstream of the sluice channel entrance was also simulated because scour in this reach controlled the sand concentration entering the sluice channel.

Sediment sizes in the deposited material were obtained from bed samples collected before and after sluicing. A range of samples collected throughout the deposit would have been more representative, so this may have introduced some inaccuracy.

Sluicing rates predicted by the numerical model depend directly on the predictions of alluvial friction and sediment transport prediction methods. These methods all employ empirical constants derived from laboratory or field measurements. The measurements usually cover a range of conditions which do not include the extreme conditions found in a settling basin during sluicing, therefore, when the methods are applied to sluicing they are being extrapolated beyond the conditions for which they were originally derived. It is wise, then, to test all the suitable friction and transport prediction methods and select the most reliable pair. The comparison between predicted and observed volume flushed from the sluice channel for each combination of prediction method is given below.

Friction prediction method	Transport prediction method	Resulting prediction of sediment volume sluiced (m^3)
Brownlie (1983)	Ackers and White (1973)	3,260
	Brownlie (1981)	3,430
	Engelund and Hansen (1967)	3,620
	van Rijn (1984)	3,240
Engelund (1966)	Ackers and White (1973)	2,210
	Brownlie (1981)	3,570
	Engelund and Hansen (1967)	4,390
	van Rijn (1984)	1,620
Observed value		2,700

Only the Brownlie (1983) and Engelund (1966) alluvial friction predictors were tried because the White et al (1979) method does not apply to flow with high Froude numbers and the van Rijn (1984) method does not simulate the increased roughness when antidunes are formed in supercritical flow.

The Engelund (1966) friction prediction method gives more varied results than the Brownlie (1983) method; this may be due to the sudden discontinuity in roughness which it predicts when the flow transfers from subcritical to supercritical. The discontinuity also made the model less stable (very short time steps were required to enable a stable simulation). Therefore the Engelund method was not used for subsequent sluicing comparisons.

The predictions of volume sluiced are good when the Brownlie friction predictor is used, predictions are within 35% for all transport prediction methods, all methods overpredict volume sluiced. The most suitable transport predictor appears to be the Ackers and White method; however, the method

has been found to overestimate sediment transport when grain sizes are less than about 0.15mm, a common condition for settling basins. The comparison with data from the Karangtalun basin, Section 3.3.3, highlights this deficiency.

The van Rijn (1984) sediment transporting predictor gave the best result of the remaining three methods. The van Rijn predictor also performed best in a study by Voogt et al (1991), they tested the van Rijn, Ackers and White and Engelund and Hansen predictors against a restricted data set for fine sand transport (0.1mm to 0.4mm) in relatively fast flowing water (up to 2.8m/s), conditions approaching those in a settling basin during sluicing. Therefore the van Rijn (1984) sediment transport predictor was used in the detailed comparisons between the sluicing model and field data which are presented below.

Figure 9 presents bed elevations in the Mae Tang sluice channel before and after sluicing. The elevations after sluicing are compared with model prediction; overall agreement is good but the overestimate in sluiced volume is seen, it appears as overpredicted scour at the upstream end of the channel. Water levels during sluicing were also measured and they are compared with the model's predictions in Figure 10; agreement is again good.

3.2 Yangwu sluiced settling basin

3.2.1 Description

The Yangwu canal is in Yuanping County, Shanxi Province, China, it carries a discharge of about $1 m^3/s$ which is taken from the Yangwu river. The irrigation canal system was suffering from sedimentation problems and so two remedial measures were adopted. Firstly, the layout of the intake to the first lateral was modified to reduce the sediment load abstracted, and secondly, a settling basin was constructed in the main canal between the first and second laterals. The settling basin site was adjacent to the Yangwu river and so there was sufficient head for sluicing the basin.

Field measurements at the settling basin were undertaken in 1982 by the Shanxi Provincial Institute of Hydraulic Research; they are reported in Ning et al (1983). The measurements cover both the deposition and the sluicing phases of operation.

3.2.2 Comparison with deposition model

The data used for input to the deposition model are presented in Table 3. The majority of the data was obtained from Ning et al (1983), but some further data was provided by personal communication with the second author.

The sand concentration entering the basin was derived from information on the composition and volume of material settling in the basin. The silt concentration, settling velocities and settled density were estimated because measured values were not available. The only effect produced by silt on the deposition pattern was at the downstream end of the basin when it was in the early part of the filling period. Figure 11 presents a comparison between predicted and observed deposition when simulation of silt is omitted. Figure 12 gives the same comparison including silt simulation using estimated values, in each case the prediction of overall behaviour is good, with inclusion of silt simulation having little effect.

It was not possible to compare the predicted sediment concentrations and sizes leaving the basin with observed values, due to a lack of data. It was also not possible to compare directly the predicted and observed deposition pattern due to a variation in sediment concentrations entering the basin, which was not measured.

A meaningful quantitative comparison that is possible is the bed slope on the sediment deposition front (the deposition front is marked on Figure 12). A correct prediction of the value of this slope is a useful verification of the model, it is also of engineering interest because it can affect the storage volume of a basin. For example at the Karangtalun basin (described in the next section) the slope is shallow, and so the basin is only partially filled when sand concentrations passing into the canal begin to rise appreciably.

The predicted and observed slope of the deposition front is plotted against position in the basin in Figure 13. Both the value of the slope and its increasing trend in the downstream direction are accurately predicted by the model. This result builds further confidence in the model's predictions.

Another quantitative comparison which can be made is the comparison between predicted and observed sediment sizes in the deposits after the basin had filled; it is shown in Figure 14. Again the agreement is good.

3.2.3 Comparison with sluicing model

The data used for input to the sluicing model are shown in Table 4. A large part of the data are predictions from the deposition model: bed levels, bed material densities and sand grain sizes in the deposit.

The value for sand concentration entering the basin during sluicing was an estimate, however the value had an insignificant effect on the predicted sluicing behaviour as sand concentrations leaving the basin were around 100 times greater.

The Brownlie (1983) friction method was used in the sluicing model in conjunction with each sediment transport predictor. The results are shown below.

Sediment transport predictor used in model	**Predicted time to sluice basin empty (Hours)**
Ackers and White (1973)	5.6
Brownlie (1981)	6.0
Engelund and Hansen (1967)	3.8
van Rijn (1984)	7.2
Measured value	7.2

The predicted sluicing times largely compare well with the measured value, the worst error is a 47% underestimate which is comparable with the half to twice error band usually associated with sediment transport predictions. The van Rijn method, which is the preferred one after comparison with data from

Mae Tang (Section 3.1.3) gives the best prediction. Other methods underestimate sluicing time.

Figure 15, a plot of volume sluiced against time, shows satisfactory agreement between prediction and measurements. Figure 16 gives a comparison between the predicted and observed water surface profiles in the basin after 0.33, 2.3 and 6.0 hours of sluicing, it shows how the predicted sluicing pattern is very similar to the observed pattern.

The predictions shown in Figures 15 and 16 were obtained by using the van Rijn sediment transport predictor in the sluicing model.

3.3 Karangtalun sluiced settling basin

3.3.1 Description

The Karangtalun settling basin is located at the head of the Mataram canal, near Yogyakarta in central Java; the canal's discharge is about 16 m^3/s. A plan view of the headworks and settling basin is shown in Figure 1. The offtake is located on the outer bank of a sharp bend of the Kali Progo river, also the cill level of the intake gates is set higher than the river bed elevation. These features minimise the entry of coarser sediments to the canal system.

Finer sediments are trapped in a settling basin, the scour sluices at the downstream end of the basin are kept partially open during normal basin operation and so some sediment is continuously passed back to the river. The basin is flushed, with the scour sluices fully open, every two weeks during the wet season and every four weeks in the dry season.

A detailed set of measurements over two complete cycles of deposition and sluicing were undertaken by HR Wallingford in collaboration with the Kali Progo Irrigation Project. Measurements were carried out in February and March 1987 and are reported in Fish (1987).

3.3.2 Comparison with deposition model

The data used for input to the model is presented in Table 5, data for both filling periods are shown.

A difficulty with the measurements was the rapid variation in the river's sediment concentration. Periods of high silt and sand entry usually occurred at night, while the monitoring was only undertaken during daytime. The routine measurements of sediment entry were therefore considered unreliable and sediment input was derived from the quantities trapped in the basin and measured leaving the basin. A constant sediment input to the basin was assumed.

The settling velocities and settled density of the silt were not measured, and so estimated values were taken in the same way as for the Yangwu basin.

A range of comparisons between the deposition model and data are shown in Figures 17 to 20. The first two of these figures show comparisons between the predicted and observed deposition patterns for the two filling periods. The overall patterns are predicted correctly; this result is especially encouraging

because the deposition pattern is very different from that found for the Yangwu basin (Fig 12).

The deposition pattern in the first 150m of the Karangtatun basin is not predicted well. However, this is of little significance because the region has only a secondary effect on the overall performance of the basin. The reason for the discrepancy is largely the deposition and re-working of sediment associated with the variation in sediment concentrations entering the basin; these variations could not be simulated due to a lack of data.

The good predictions of total deposited volume in the basin after each filling period is not a verification of the model. The mean quantities of sand and silt entering the basin were derived from the deposited volumes.

Predicted sand concentration entering the canal is an important quantity for comparison with data because it is the principal measure of a basin's performance. At the Karangtalun basin the sand concentrations entering the canal are a little less than those actually leaving the basin because the scour sluices divert the bottom region of the flow back to the river. The deposition model predicts variations in concentration with height above the bed, so it was able to simulate the effect of the scour sluices on sand concentrations entering the canal.

A comparison between predicted and observed sand concentration entering the canal is presented in Figure 19; agreement is good. There is some scatter for the first filling period but it is small compared to the mean sand concentration entering the basin. The maximum discrepancy between predicted and observed sand concentration passing into the canal was only 13% and 2% of the mean concentration entering for the two filling periods. The scatter is due to the variation in sand concentration entering the basin, which was not measured.

Another quantitative comparison between prediction and measurement is shown in Figure 20, where sand grain sizes within the deposit are presented. The predictions are accurate.

3.3.3 Comparison with sluicing model

The data used for input to the sluicing model are shown in Table 6. A large part of the data are predictions from the deposition model, in the same way as for the simulation of sluicing at the Yangwu basin. The sand concentration entering the basin during sluicing was not measured, a mean of measured values from other days was used. The value chosen for sand concentration entering the basin had an insignificant effect on the predictions, because it was a tiny fraction of the concentrations leaving the basin.

Similarly to the other sluicing predictions, the Brownlie (1983) alluvial friction prediction method and van Rijn (1984) sediment transport prediction method were used in the sluicing model. However, the table below is presented to demonstrate how the van Rijn predictor compares with the other methods.

Sediment transport predictor used in sluicing model	Resulting prediction of time to sluice basin empty (hours) 24.2.87 Sluicing	10.3.87 Sluicing
Ackers and White (1973)	0.42	0.52
Brownlie (1981)	1.47	1.15
Engelund and Hansen (1967)	1.25	0.99
van Rijn (1984)	1.63	1.28
Measured value	1.83	1.50

These results confirm that the Ackers and White method overestimates sluicing rates when the sand sizes are small (the median sand size entering the basin during deposition was 0.135mm). Predictions using the van Rijn sediment transport method were again the most accurate.

The van Rijn method is confirmed as the most reliable for all three sites, and for the comparison against sediment transport data reported by Voogt et al (1991), which covered conditions similar to basin flushing (see Section 3.1.3).

Predicted volumes sluiced from the basin are compared with observation in Figure 21; agreement is good. However, a discrepancy was found between predicted and observed sand concentrations leaving the basin; predictions were in excess of twice measured values. The most likely explanation appears to be that the measured concentrations, which were sampled from near the surface, were much less than the depth averaged concentrations. An inconsistency between the measured concentrations and measured sand volumes sluiced from the basin adds support to this explanation.

3.4 Canals of the Gezira Irrigation Scheme

The Gezira Irrigation Scheme in Sudan irrigates 880,000 hectares using water drawn from the Blue Nile. Land slopes are low and sediment concentrations in the Blue Nile have increased significantly since the scheme's construction in the 1930's. Severe sedimentation has occurred in both the major canals (with discharges of a few cubic meters per second) and the minor canals (with discharges of around 0.2 m^3/s). The deposited material consists of silts and clays.

A sediment monitoring programme was undertaken by the Sudan government's Hydraulics Research Station, Wad Medani, the work formed part of the World Bank's Sudan Gezira Rehabilitation Project, it is described in HR Wallingford (1991). Measurements included bed material sampling, current metering, suspended sediment sampling, stage records, bed level surveys and measurements of settling velocity.

The data was used to validate the sediment deposition model for Gezira conditions, so that the model could be used to test basin design options for the scheme. Comparisons were made between predicted and observed sediment concentrations leaving the first reach of four canals where sedimentation was severe. Canal headreaches were chosen for the comparisons because they

were producing the same effect as settling basins: trapping large volumes of sediment. Comparisons were made over a season, at the start of the irrigation season concentrations entering the canals were high and bed accretion was rapid, by the end of the season the concentrations entering the canals had dropped to around 200ppm and very little of this material was depositing.

The constant in the Westrich and Jurashek equation (Equation 23) was set using the Gezira data, as outlined in Section 2.1.6, no other calibration of the model was employed.

Input data to the model included measured bed levels at the start of the irrigation season, weekly averaged sediment concentrations and weekly averaged discharges. Because the canals did not have sand beds an alluvial friction predictor could not be used, therefore measured roughness values were taken. Comparisons were conducted for a season's data.

Good agreement was found between predicted and observed concentrations leaving the canal reaches, the comparisons are given in Figures 22 and 23. These results are of particular interest because they form the only field validation for the model's predictions of silt deposition.

3.5 Summary of field verification and performance of other methods

3.5.1 Deposition

Table 7 presents a summary comparison between the field data described in this Chapter and existing methods for settling basin design. The results of the deposition model are also included in the table. Existing methods predict basin performance at an instant, rather than variations in performance with time, so comparisons are given in Table 7 at the start and at the end of the filling process. The existing methods do not predict the deposition patterns within a settling basin, so they cannot be used to determine depths or widths in a basin as it fills. Therefore the depths for input to the existing design methods were taken from the predictions of the deposition model, mean widths were derived from the known water surface widths, the predicted depths and the basin side slopes.

Data from the Gezira canals is not included in Table 7, its comparison with the design methods is presented in Table 8.

Existing methods do not give accurate predictions of basin performance: Vetter's and Camp's methods overestimate basin performance, while the method of Garde et al underestimates performance. The Garde et al method does give good predictions for the Gezira canals, but Vetter's and Camp's methods still overestimate sediment trapping.

The depositional model gives more consistently reliable results: both the predicted sediment concentrations leaving the sand traps (or Gezira canal reaches) and the changes in the concentration as a basin fills are predicted accurately.

Figures 8, 11 to 14, 17 to 20, 22 and 23 compare predictions from the deposition model with field data from a sluice channel, two settling basins and

four canal reaches, overall they show very good agreement between model predictions and field data. The comparisons include concentrations down a channel, patterns of deposition, sediment sizes in deposited material and sediment concentrations leaving a basin.

3.5.2 Sluicing

There are no existing methods specifically developed for predicting sediment sluicing from a settling basin, (an example of present practice is the application of sediment transport predictors to the flow in an empty basin to derive a design case sluicing rate, Avery, 1989, p92). So this section will summarise only the comparison between the sluicing model and field data.

A summary of the comparison is presented below.

Site	Time required to sluice basin empty (hrs)	
	Observed	Predicted
Mae Tang *	3.0	1.1
Yangwu	7.2	7.2
Karangtalun		
24.2.87	1.8	1.6
10.3.87	1.5	1.3

Note: * A sluice channel, so it could not be flushed empty. Values shown are times to sluice 2,700m^3 from channel.

These results show how the sluicing model predicted sluicing behaviour at three field sites with good reliability. More detailed comparisons are shown in Figures 9, 10, 15, 16 and 21, which show predicted and observed sluicing rates and sluicing patterns.

Where discrepancies between the sluicing model and measurements did occur, they showed the sluicing model underpredicting sluicing time. A factor of safety on predicted sluicing time therefore appears necessary when the method is to be used for design.

4 Other aspects of settling basin design

The models described in Chapter 2 do not cover every aspect of settling basin design because they assume width averaged conditions. In particular the design of the entry to a basin cannot be assessed by the models.

This chapter discusses the effect of the basin entry, and the maximum width that a basin can have without causing operational problems. The design of outlet structures and escape channels are also briefly discussed.

4.1 Design of basin entry

The purpose of a well designed basin entry is to convey the flow with relatively fast velocities in the reach upstream of the basin into the slower flow within the

basin, without causing excessive turbulence or flow separation. Turbulence causes mixing and so hinders settling, while an excessive flow separation will cause parts of the basin to become dead zones which are by-passed by the flow.

The computational fluid dynamics model used to predict the additional turbulence produced by deepening flow in a basin (Section 2.1.3) can also be applied to the flow at a basin's inlet. This section describes how the modelling has been used to derive design recommendations for a standard entry geometry.

We assume initially that there is a straight conduit or canal reach upstream of the settling basin. The transition from the narrower upstream reach to the basin's width is then affected by means of a simple expansion, see Figure 24. Existing designs and design recommendations usually employ expansion rates ranging from 1:5 to 1:10, where the expansion rate is the width increase at each bank per metre of downstream distance (Figure 24).

Simulations using the computer model were performed for a range of basin entry geometries and hydraulic conditions. The range of values is given below:

Width ratio, W_b/W_u	: 2 to 4
Depth ratio, h_b/h_u	: 0.5 to 2.5
Relative roughness height, k_s/h_u	: 0.005 to 0.125
Channel aspect ratio, W_u/h_u	: 5 to 50
Expansion rate	: 1:0 (abrupt expansion) to 1:20
Channel side slope	: 1:0 (vertical sides) to 1:1.5

where W_u is channel bed width upstream of the basin,
W_b is basin bed width,
h_u is depth in upstream channel,
h_b is basin depth at the outlet of the expansion, and
k_s is bed roughness height.

The simulations of basin entries showed that the additional turbulence caused by an entry was in most cases small when compared to turbulence levels for uniform flow in the basin. A more significant effect was the non-uniform lateral distribution of flow, velocities at the basin centreline could be more than twice the mean velocity. Clements (1966) has shown that velocity variations across the width of a basin affect trapping efficiency considerably more than velocity variations in depth. Therefore an upper limit to the ratio of u_c, the depth averaged centreline velocity, to $\bar{u}$, mean velocity (defined as discharge divided by flow area), was selected as the criterion for design. The value chosen for the upper limit was $u_c/\bar{u} = 1.5$.

Figure 25 shows a plot of the ratio $u_c/\bar{u}$ against expansion rate, E, for various conditions.

For each set of conditions the expansion rate at which $u_c/\bar{u} = 1.5$ was found using plots similar to Figure 25, this limiting expansion rate can be termed E_l. E_l was found to vary strongly with the width ratio, depth ratio, relative roughness and channel aspect ratio, however a non-dimensional number

which incorporated all these efects was found to have a consistent relationship with E_l. The non-dimensional number was the ratio of forces R_f:

$$R_f = \frac{\text{bed friction force in the basin}}{\text{momentum of the flow approaching expansion}} \qquad (28)$$

The ratio is defined for a flow streamline at the centre of the channel, see Figure 24. The friction force is derived from the bed shear summed over a specified distance in the direction of the flow, this distance is taken as a factor of the upstream bed width, W_u. The momentum, meanwhile, is the product of velocity and mass flow per m width, which has units N/m. If the concept of continuity is used to relate the flow velocities upstream of the expansion to those downstream we obtain:

$$R_f = \frac{1.5\ W_u}{A_r\ f^2\ h_b} \qquad (29)$$

where A_r is the ratio of cross section area downstream from the expansion to that upstream, and

f is the friction factor, defined as $\bar{u}/u_*$, in the basin downstream from the expansion.

A plot showing how E_l was related to R_f for all the conditions modelled is given in Figure 26, there is a slight scatter overlying the trend, this scatter reflects the fact that the situation being modelled is too complex for E_l to be related perfectly to just one non-dimensional number. The points on Figure 26 can be used to derive a design relationship, a curve has been fitted to the upper boundary of the scatter, it yields the design equation:

$$E_l = \frac{A_r\ f^2\ h_b}{6\ W_u} \qquad (30)$$

Equation (30) would be used by first calculating f from the conditions at the upstream end of the basin and then A_r from the dimensions of the approach channel, Equation (30) then yields a minimum value for the expansion rate E.

If E_l is unacceptably large then a submerged weir might be tried, see Figure 24, this would cause a reduction in both h_b and A_r (together with a small rise in f). However, the derivation of the ratio R_f includes a length scale, W_u, which is assumed to be related to the distance over which the friction force at the upstream end of the basin is acting. If a submerged weir is adopted then this distance will be related to its crest length, so a crest length must exceed a minimum value for Equation (30) to apply. Tests using the computational model showed that the crest length should exceed half of W_u if Equation (30) is to be used.

Another way of adjusting an entry design when E is too large is the inclusion of vanes in an expansion. A recommended design incorporating vanes is shown in Figure 27, it has been taken from a guide to internal flow systems (Miller, 1978).

Equation (30) has been derived using simulations of flow at basin entry sections where the approach condition was a straight channel, such conditions may not in general apply at a settling basin. For complex geometries, such as

combinations of gates, expansions and submerged weirs, hydraulic modelling or numerical modelling would be recommended. However additional simulations with the following approach conditions were performed:

(i) a 90° channel bend ending at one channel width upstream from the expansion, the curvature of the bend was very tight, radius of curvature was similar to the channel width, the approach channel was divided into two by a central divide wall, and

(ii) an undershot gate situated one channel width upstream from the expansion, gate opening was 30% of flow depth.

When Equation (30) was used to set E for these conditions, the predicted ratio of maximum velocity to mean velocity was 1.44 for case (i) and only 1.07 for case (ii), so safe designs were obtained.

A prediction of the additional turbulent viscosity at the upstream end of a basin, ν_{to}, is required for input to the deposition model. The results of the simulations suggest low values of additional turbulence, so an approximate method is acceptable. For designs prepared using Equation (30) the following relationships can be used, if the expansion has no bed slope, or the bed rises:

$$\nu_{to} = 0.01 \frac{Q}{W_b} \qquad (31)$$

where Q is the design discharge during normal basin operation (m^3/s).

If deepening as well as widening is employed at the entry then additional turbulence is produced. Using Equation (3) from Section 2.1.3 in combination with Equation (31):

$$\nu_{to} = 0.01 \frac{Q}{W_b} + (0.0015 + 0.13\, S_{be}) \frac{Q}{W_u} \qquad (32)$$

where S_{be} is the bed slope of the entry section.

4.2 Maximum width for deposition

If a basin has a well designed entry then the flow and sediment should be evenly distributed across the basin, so bed levels should also rise evenly across the basin as it fills. We might therefore expect to find no width limitation for a basin. However if the upstream part of a basin fills completely, so that a channel of natural width forms within it, then a transition from this natural width to the full width of the basin will be produced. This natural transtion is likely to be relatively abrupt, so it may produce excessive turbulence and flow separation if the increase in width is large. Therefore a criterion for setting the maximum allowable width for a basin is required.

A limit must be set on the ratio between the natural channel width and the basin width so that large recirculating zones and hence high values of $u_c / \bar{u}$ are avoided. If the ratio of downstream to upstream width at the natural expansion is kept to a maximum of 1.5, then even relatively abrupt expansion rates will be acceptable. Therefore we can recommend a maximum allowable

basin width for deposition of 1.5 times the stable alluvial width. If the well known Lacey (1930) regime width predictor is adopted, then the criterion becomes:

$$W_{dmax} = 7.2\,Q^{0.5} \qquad (33)$$

where W_{dmax} is the maximum allowable width for the deposition phase of basin operation (m), and

Q is the design discharge during normal basin operation (m^3/s).

The criterion above is only necessary when the upstream part of the basin is allowed to fill completely, so exceptions can apply. For example desilting procedures in a continuously dredged basin may be set so that a natural width channel cannot start to form.

4.3 Maximum width for sluicing

If a basin is made excessively wide compared to its sluicing discharge, then the flow is likely to cut a narrow valley through the sediment deposits in the basin. This will leave sediment berms in the basin after flushing and so greatly reduce sediment storage. A basin which is to be flushed should therefore have a width that does not exceed the natural width of its sluicing flow.

4.3.1 Laboratory investigation of sluicing width

The maximum allowable sluicing width could simply be set at the stable width predicted by Lacey's or another regime method. However, the data from which these methods have been developed do not cover the extreme conditions found in settling basins during flushing. There are two principal differences between conditions in natural channels flowing in regime and those in sluiced settling basins. Firstly the slopes and sediment concentrations in basins are much greater, secondly flushing durations are only hours or less while the data used for regime methods was collected from channels which had stabilised after months or years.

To investigate the importance of these differences a set of tests were performed in a laboratory scale settling basin. The basin layout is shown in Figure 28, its length was 16m and width 5.3m. Initially the basin was levelled to form a shallow slope down the basin. Before each test a channel was cut down the centre of the basin to encourage the sluicing flow to take a straight path, the width of this channel was much less than the width eventually formed by the flow.

Tests at three discharges were performed, for each test the widths steadily increased as sluicing progressed and were still increasing when the test was completed. A test was considered complete when the flow first began to show signs of meandering, in a prototype basin meandering is prevented, and so the results would not have been representative if the tests were continued. The completion of a test before the bed widths in the basin had reached their minimum possible values produced a degree of safety in the results, because widths were still rising even at test completion.

4.3.2 Results and interpretation

The results of the experiments just described are shown in the table below.

Test No	Discharge (m^3/s)	Mean Slope	Duration (mins)	Mean Width (m)
1	0.0032	0.021	40	0.77
2	0.016	0.014	94	1.20
3	0.026	0.009	150	1.90

Most regime relationships for channel width relate the width to discharge and to no other parameter. Therefore the results shown above are plotted on a graph of width against discharge, Figure 29. Also plotted on the graph are the laboratory data of Ranga Raju et al (1977) and a line fitted by Ackers to 30 data points collected during experiments on stable streams in alluvium (Ackers, 1964). The details of all the data shown on Figure 29 are given in Table 9. The figure shows that the widths produced by sluicing are comparable or larger than those observed at equivalent stable alluvial channels of mild slope. We conclude therefore that we can apply regime width predictors to the conditions in settling basins during sluicing.

The Lacey method for width prediction can be used for determining the maximum width in a settling basin during flushing:

$$W_{smax} = 4.83\, Q_s^{0.5} \qquad (34)$$

where W_{smax} is the maximum allowable width for sluicing (m), and
Q_s is the flushing discharge (m^3/s).

Equation (34) is plotted onto Figure 29, it underpredicts width for the discharges shown on the graph. This may appear to introduce a further factor of safety, but at the higher discharges common to prototype settling basins Lacey's method does not underpredict widths.

4.4 Implication of width predictions on basin design

Two criteria for determining the maximum allowable basin width have been presented, Equations (33) and (34). The design sluicing discharge may exceed the design discharge during normal operation, so the criteria can in some circumstances produce similar recommendations. However when these discharges are equivalent the maximum deposition width will be 50% more than maximum allowable width for sluicing.

It can be possible to set both the deposition and sluicing widths at their maximum, by designing a basin with sloping sides. The sluicing width is then less than deposition width because water levels are lowered during sluicing, while deposition width applies to the flow in a near full basin.

However, there is a minimum to the side slope of a basin, low slopes will allow small berms to form above the water surface when the basin is being flushed and is nearly empty, while higher slopes will cause these berms to slump

down into the water. The critical side slope is difficult to predict because it will depend on the soil properties of the material deposited. Critical slopes can range from near horizontal for poorly consolidated silt deposits, to near vertical for sand which has developed negative hydrostatic pore pressures.

Therefore, when the near-full width of a basin is set greater than the sluicing width, engineering judgement must be employed in the selection of a side slope. If, however, the near-full width is determined from sluicing width then any convenient side slope can be selected.

4.5 Outlet structures and escape channel design

The design of the outlet layout from a basin will only significantly affect basin performance through its effect on water levels in the basin. Turbulence levels or the velocity distribution at an outlet do not affect the flow upstream from a very localised region.

The effect of the water level produced by an outlet structure is a dominant factor in basin performance during both the deposition and the sluicing phase of operation, predictions using the numerical models would be used to quantify the effect and hence aid the design of an outlet. For example, an outlet design in a sluiced basin would usually incorporate a weir or set of gates to control the water level during normal basin operation, and a low level gated outlet for sluicing. There is a need to lower water levels during sluicing as low as possible, but this will lead to a large and hence expensive outlet structure. A compromise design can be derived by means of hydraulic calculations on the outlet layout and simulations using the numerical models.

An escape channel from the low level outlet to a sediment discharging point may be required, (the point would usually be in the river from which the water was originally abstracted). If an escape channel is to be used then its sediment input, predicted by the sluicing model, would need to be checked against predictions of the channel's sediment transporting capacity.

5 Conclusions

This report has presented the development and field verification of two numerical models for predicting settling basin performance. The first model predicts the deposition behaviour and hence the concentration and sizes of the sediment leaving a basin throughout its filling process. The prediction allows a basin's filling time to be determined, and hence the required frequency of flushing. The second model predicts sluicing rates, and hence the time required to empty a basin by gravity flushing.

Field verification of the deposition model has included comparisons between the model's predictions and measurements of sediment deposition patterns, sediment sizes in deposited material and concentrations passing downstream of the settling reach. Field data have been obtained from settling basins, a sluice channel and canal reaches of an irrigation scheme where severe silt deposition occurs. Good predictions were obtained for each site.

Existing settling basin design methods were also compared with the field data. Only predictions of concentration leaving a basin or settling reach could be

compared with data, and then only for an instant, because existing methods do not predict how concentrations leaving a basin change as the basin fills. Predictions of the existing methods did not agree well with the measured data: Vetter's and Camp's methods overestimated sediment trapping while the method of Garde, Ranga Raju and Sujudi largely underestimated sediment trapping.

Field verification of the sluicing model used data from two settling basins and a sluice channel. Good predictions of sluicing rates and sluicing patterns were found, but where discrepancies between measurement and prediction did occur the model underestimated sluicing time. A factor of safety on the predicted time to flush a basin is therefore recommended.

The models described in this report would benefit from further field verification because they have, to a certain extent, been developed using the data presented in Chapter 3. In particular both the deposition and sluicing models use predictions of alluvial friction and sediment transport, a range of methods are available for these predictions and the ones producing the best overall predictions were adopted in each model. Also the predictions of silt movement within the deposition model have only been verified with field data from the Gezira irrigation scheme. Those data were used to set a constant in the silt transport prediction formula, on which predictions of silt deposition depend.

Meanwhile, the new methods are a significant improvement on present practice (Section 3.5) and so publication of a new design procedure for settling basins is planned. An outline procedure is given in the Appendix. The models for deposition and sluicing prediction both use the assumption of uniform conditions across the width of a basin. The models therefore cannot be used to set the width of a basin or design its entry. A separate study of these aspects of basin design was undertaken, and the results are included in the design procedure.

6 Acknowledgements

This report was prepared in the Sediment Control Section of the Overseas Development Unit at HR Wallingford. The Unit is headed by Dr K Sanmuganathan.

The study is funded by the British Overseas Development Administration.

The computer package for flow simulation which was used in this study was the 'PHOENICS' code supplied by CHAM Ltd of London.

7 References

Ackers P, 1964. Experiments on small streams in alluvium, Proc ASCE, Vol 90, HY4, July 1964.

Ackers P and White W R, 1973. Sediment transport: new approach and analysis. ASCE, Journal of the Hydraulics Division, No HY 11.

Adams E W and Rodi W, 1990. Modelling flow and mixing in sedimentation tanks. ASCE Journal of Hydraulic Engineering, Vol 116 No.7.

Atkinson E, 1986a. A model for the design of sluicing type sediment control structures. Report No ODTN 18, HR Wallingford, UK.

Atkinson E, 1986b. The performance of diversion weirs in rivers carrying high sediment loads. Final report on a field study in Northern Thailand. Report No OD 86, HR Wallingford, UK.

Atkinson E, 1987. Field verification of a performance prediction method for canal sediment extractors. Report No OD 90, HR Wallingford, UK.

Atkinson E, 1989. Predicting the performance of sediment control devices at intakes. Report No ODTN 41, HR Wallingford, UK.

Avery P (editor), 1989. Sediment control at intakes - a design guide. British Hydromechanics Research Association, Cranfield, Bedford, UK.

Bechteler W and Schrimpf W, 1983. Mathematical model of non-uniform suspended sediment transport. Proc Second International Symposium on River Sedimentation, Nanjing, China.

Bettess R and White W R, 1979. A one-dimensional morphological river model. Report IT 194, HR Wallingford, UK.

Brownlie W R, 1981. Prediction of flow depth and sediment discharge in open channels. W M Keck Laboratory of Hydraulics and Water Resources, California Institute of Technology. Report KH-R-43.

Brownlie W R, 1983. Flow depth in sand bed channels. ASCE Journ Hydr Eng Vol 109 No 7.

Camp T R, 1946. Sedimentation and the design of settling tanks. Paper 2285 Trans ASCE Vol 111.

Clements M S, 1966. Velocity variations in rectangular sedimentation tanks. Proc. ICE, Vol 34, p171.

Dobbins W E, 1944. Effect of turbulence on sedimentation. Paper 2218 Trans ASCE Vol 109.

Engelund F, 1966. Hydraulic resistance of alluvial streams. Proc ASCE Vol 92, HY 2.

Engelund F and Hansen E, 1967. A monograph on sediment transport. Technisk Forlag, Copenhagan.

Fish I L, 1987. Field measurements at Karangtalun sluiced settling basin, Yogyakarta, Central Java, Indonesia. Report No ODTN 31, HR Wallingford, UK.

Garde R J, Ranga Raju K G and Sujudi A W R, 1990. Design of settling basins. Journal of Hydraulic Research, Vol 28, No 1, p81.

Gibbs R J, Matthews M D and Link D A, 1971. The relation between sphere size and settling velocity. Journ of Sedimentary Petrology Vol 41, No 1.

Hazen A, 1904. On sedimentation. Trans ASCE Vol LIII, p63.

HR Wallingford, 1991. Siltation problems in the Gezira Irrigation Scheme, Sudan. ODU Bulletin No. 21, January 1991, HR Wallingford, UK.

Kerssens P J M, Prins A and van Rijn L C, 1979. Model for suspended sediment transport. Journal of Hydraulics Division, ASCE, Vol 105, No HY5.

Lacey G, 1930. Stable channels in alluvium. Minutes of Proc. ICE, 229, p259-384, London, UK.

Lane E W and Kalinske A A, 1942. Engineering calculations of suspended sediment. Trans Am Geophysical Union, 22.

Meadowcroft I C, 1988. The applicability of sediment transport and alluvial friction prediction formulae to irrigation canals. Report ODTN 34, HR Wallingford, UK.

Molinas A and Yang C T, 1985. Generalised water surface profile computations. Journ of Hydr Eng, ASCE, Vol 111, No 3.

Ning Q, Bin Z, Fengquan X, Zhijun R and Zhixiang W, 1983. Application of the experiences obtained from the Yangwu irrigation district in dealing with the sediment problem of low-head diversion works. Journal of Sediment Research, Beijing, China, No 2 (in Chinese, English translation at HR Wallingford).

Ranga Raju K G, Dhandapani K R and Kondap D M, 1977. Effect of sediment load on stable sand canal dimensions. ASCE, Journ. of Waterway, Port, Coastal and Ocean Division, Vol 103, No WW2, May 1977.

Rodi W, 1984. Examples of turbulence-model applications. In: Turbulence models and their applications, Vol 2 by B E Launder, W C Reynolds, W Rodi, J Matthew and D Jeandel. Editions Eyrolles, Paris, France.

van Rijn L C, 1984. Sediment transport. ASCE Journ of Hydr Eng Vol 110 Nos 10, 11 and 12.

Vetter C P, 1940. Technical aspects of the silt problem on the Colorado River, Civil Engineering, Vol 10, No 11, p698-701.

Voogt L, van Rijn L C and van den Berg J H, 1991. Sediment transport of fine sands at high velocities. ASCE Journ. of Hydr. Engineering, Vol 117, No 7.

Westrich B and Jurashek M, 1985. Flow transport capacity for suspended sediment. Presented at the 21st Congress IAHR, Melbourne, Australia.

White W R, Paris E and Bettess R, 1979. A new general method for predicting the frictional characteristics of alluvial streams. Report No IT 187, HR Wallingford, UK.

Tables

Table 1: Data used for input to deposition model, Mae Tang data

Sluice channel length	170m
Side slope in sluice channel	2.0 : 1

Initial bed elevations and bed width:

Distance from inlet (m)	Bed elevation (m)	Bed width (m)
0	345.76	21.5
50	345.57	20.8
135	345.17	19.2
160	345.06	9.0
170	345.01	8.9

Discharge	21.9 m^3/s
Stage at downstream end	347.37m
Total sand concentration entering sluice channel	251 ppm
Specific gravity of sediment	2.65
Water temperature	28°C

Sand size fractions of material entering channel (mm):

D_0	0.063
D_5	0.070
D_{15}	0.086
D_{25}	0.103
D_{35}	0.119
D_{45}	0.138
D_{55}	0.166
D_{65}	0.200
D_{75}	0.234
D_{85}	0.279
D_{95}	0.380
D_{100}	1.100

Table 2: Data used for input to sluicing model, Mae Tang data

Sluice channel length	200m
Side slope in sluice channel	1 : 1.5

Initial bed elevations:

Distance from inlet (m)	Bed elevation (m)
0	345.89
36	345.71
56	345.36
82	345.17
96	345.21
112	345.16
125	345.08
135	345.12
148	345.10
167	345.13
200	345.7

The bed widths were compatible with a width of 11m at the elevation of the scour protection (343m) and the side slope of 1 : 1.5.

The simulation also required bed level and width data from the river upstream of the sluice channel entrance:

Distance upstream from sluice channel entrance (m)	Initial bed elevation (m)	Initial bed width (m)
50	346.3	55
100	346.5	54
200	346.4	38
400	346.5	29

Discharge	23 m^3/s
Stage at downstream end	344.25m
Total sand concentration in river upstream of reach affected by the sluicing	60ppm

Table 2 (continued)

Specific gravity of sediment	2.65
Density of settled sediment	1.4 tonnes/m^3

Sand size grading curve of material settled in sluice channel and in river bed upstream:

	Size in sluice channel (mm)	Size in river bed upstream (mm)
D_{35}	0.32	0.6
D_{50}	0.49	0.75
D_{65}	0.73	0.90
D_{90}	1.60	2.0

Insignificant silt quantity in deposited material

Water temperature	24°C
Duration of sluicing	3 hours

Table 3: Data used for input to deposition model, Yangwu data

Settling basin length	250m
Side slope in settling basin	1 : 0.39

Dimensions of basin:

	Elevation of concrete bed (m)	Bed width (m)
Upstream end	917.22	2.0
Downstream end	915.55	2.0

Mean discharge through basin	1.02 m^3/s
Stage at downstream end	919.2m
Mean sand concentration entering basin	400 ppm
Specific gravity of sand	2.65
Density of settled sand	1.4 tonnes/m^3
Water temperature	30°C

Sand size fractions of material entering basin:

D_0	0.063mm
D_5	0.100mm
D_{15}	0.138mm
D_{25}	0.175mm
D_{35}	0.216mm
D_{45}	0.259mm
D_{55}	0.298mm
D_{65}	0.347mm
D_{75}	0.420mm
D_{85}	0.540mm
D_{95}	0.840mm
D_{100}	1.500mm

Table 4: Data used for input to sluicing model, Yangwu data

Settling basin length	250m
Side slope in settling basin	1 : 0.39

Dimensions of basin

	Elevation of concrete bed (m)	Bed width (m)
Upstream end	917.22	2.0
Downstream end	915.55	2.0

Bed elevations in basin before sluicing: predictions from deposition model used

Mean discharge	1.1 m^3/s
Stage at downstream end	916.05m
Mean sand concentration entering basin	600 ppm (estimated)
Specific gravity of sand	2.65

Density of settled sand/silt mixture and sand size fractions of material in basin: predictions from deposition model used.

Water temperature	30°C

Table 5: Data used for input to deposition model, Karangtalun data

Data shown is for 10th to 24th February filling period, data for the 24th to 10th March period is shown in brackets where it differs from the first data set.

Settling basin length	500m
Side slope in settling basin	1 : 1

Dimensions of basin:

	Elevation of concrete bed (m)	Bed width (m)
Upstream end	153.38	12.2
Downstream end	150.97	12.2

Mean discharge through basin	19.3 m^3/s (20.7)
Mean discharge through scour sluices	3.4 m^3/s (4.9)
Stage at downstream end	155.01m
Mean sand concentration entering basin	293 ppm (164)
Specific gravity of sand	3.62
Density of settled sand	1.4 tonnes/m^3
Water temperature	27°C

Sand size fractions of material entering basin:

D_0	0.063mm
D_5	0.078mm
D_{15}	0.096mm
D_{25}	0.107mm
D_{35}	0.120mm
D_{45}	0.130mm
D_{55}	0.140mm
D_{65}	0.149mm
D_{75}	0.162mm
D_{85}	0.194mm
D_{95}	0.310mm
D_{100}	0.680mm

Table 6: Data used for input to sluicing model, Karangtalun data

Data shown applies to both the 24th February and 10th March sluicing.

Settling basin length	500m
Side slope in settling basin	1 : 1

Dimensions of basin

	Elevation of concrete bed (m)	Bed width (m)
Upstream end	153.38	12.2
Downstream end	150.97	12.2

Bed elevations in basin before sluicing: predictions from deposition model used

Mean discharge through basin	24 m^3/s
Stage at downstream end	151.9m
Mean sand concentration entering basin	50 ppm
Specific gravity of sand	3.62

Density of settled sand/silt mixture and sand size fractions of material in basin: predictions from deposition model used.

Water temperature	27°C

Table 7: Comparison between deposition prediction methods and field data

Data set	Measured sand concentration entering canal (ppm)	Predicted sand concentration (in ppm) entering canal using the method due to: Vetter (1940)	Camp (1946)	Garde et al (1990)	New Method
Mae Tang	72	30	26	144	60
Yangwu:					
Start of filling period	NA	0	0	31	0
End of filling period	NA	0	0	212	195
Karangtalun**					
February measurements:					
Start of filling period	4	1	0	142	2
End of filling period	31*	1	0	209	61
Karangtalun**					
March measurements:					
Start of filling period	3	1	0	84	2
End of filling period	14*	1	0	103	13

Notes: NA data not available

* Refer to Figure 19, data showed some fluctuations

** The tunnels at the downstream end of the basin reduced further the concentrations entering the canal. Vetter, Camp and Garde et al do not account for this so they should give slight overestimates.

Table 8: Comparison between deposition prediction methods and Gezira canal data

Data set	Measured silt concentration leaving first reach of canal (ppm)	Predicted silt concentration (in ppm) leaving the reach using method due to: Vetter (1940)	Camp* (1946)	Garde et al (1990)	New Method
Zananda Major:					
At peak concentration	4353	686	744	5278	4220
End of season	185	16	17	104	122
Gamusia Major:					
At peak concentration	4273	1895	2175	4470	4272
End of season	194	55	58	148	162
Kab el Gidad Major:					
At peak concentration	2174	342	383	2505	1326
End of season	193	47	49	181	205
Hamza Minor:					
At peak concentration	3668	590	581	3951	3233
End of season	137	15	13	206	207

Notes: * The input data lay out of the range of Camp's curves so extrapolation of the curves was used to make the predictions.

Table 9: Observations of stable width in laboratory scale alluvial channels: range of conditions

Data Source	Discharge Range (m^3/s)	Slope Range	D_{50} Sediment Size Range (mm)	Range of Test Durations (hours)
Ackers (1964)	0.01 to 0.15	0.0004 to 0.003	0.16 to 0.34	"few hours" to "few days"
Ranga Raju et al (1977)	0.018 to 0.02	0.0007 to 0.003	0.27*	20 to 80
Present data	0.003 to 0.03	0.009 to 0.021	0.16*	0.67 to 2.5

* Single sediment size used

Figures

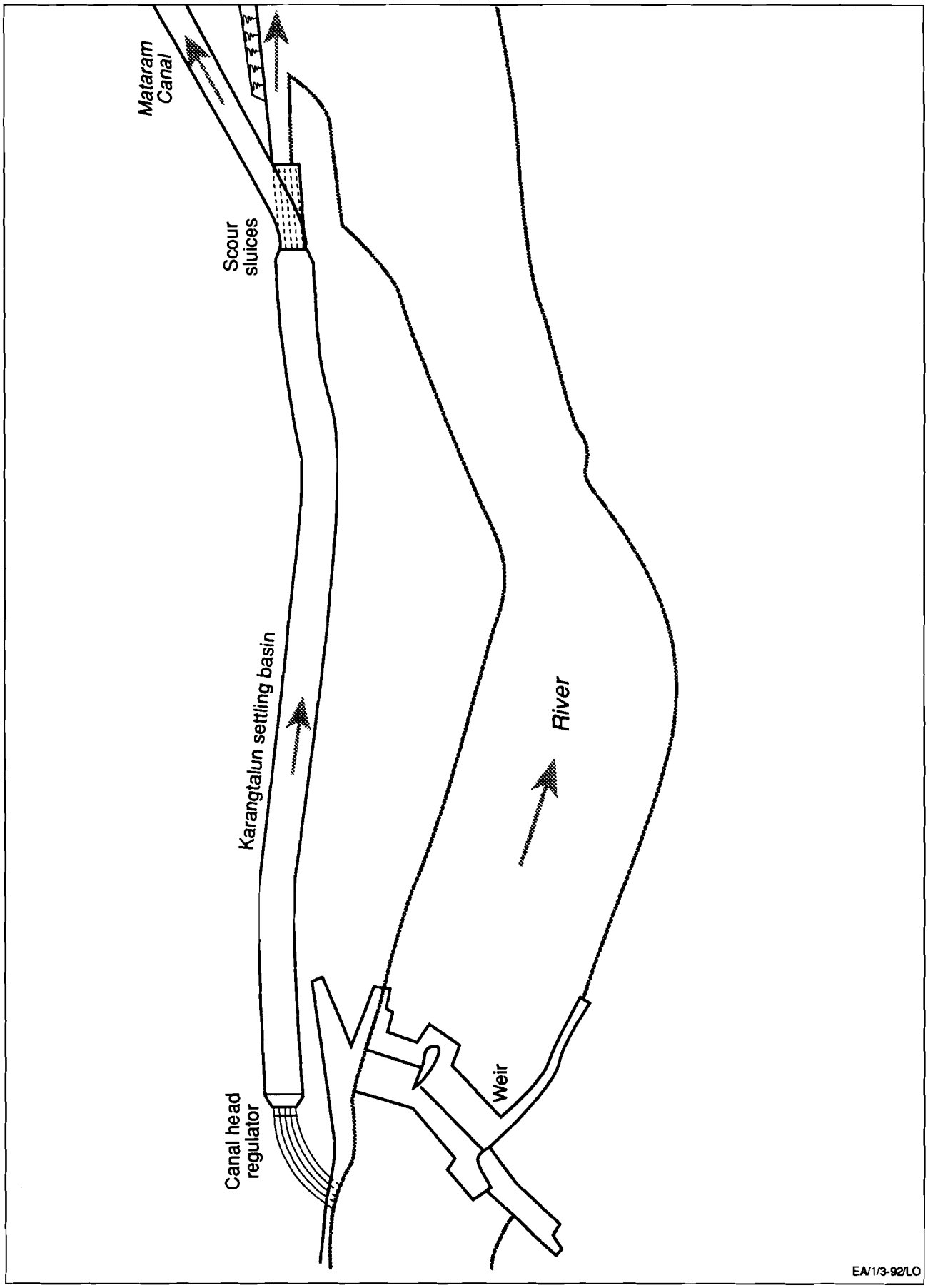

Figure 1 Mataram Canal Headworks, Java, an example of a sluiced settling basin

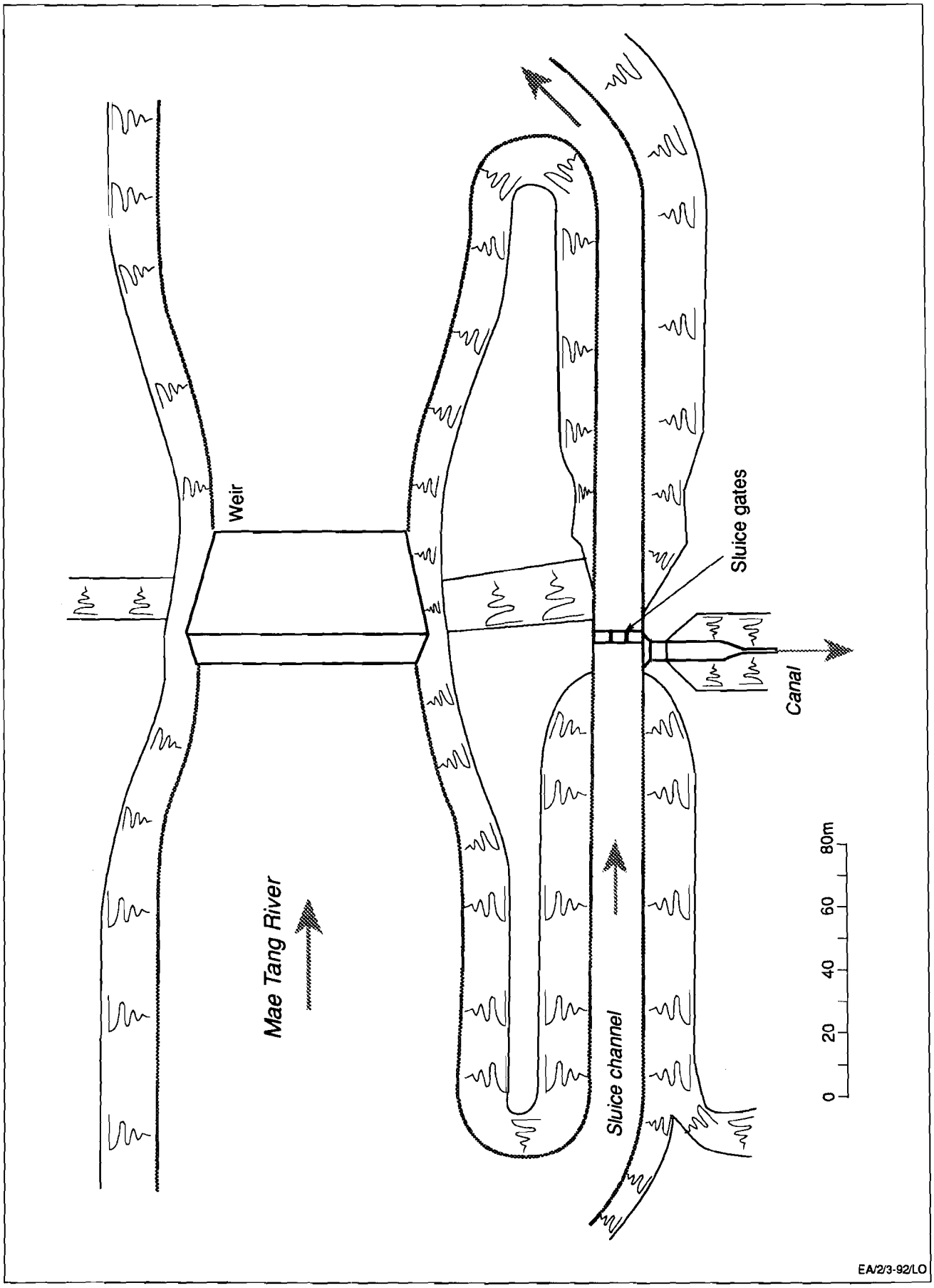

Figure 2 Mae Tang Weir and headworks, an example of an intake with a sluice channel

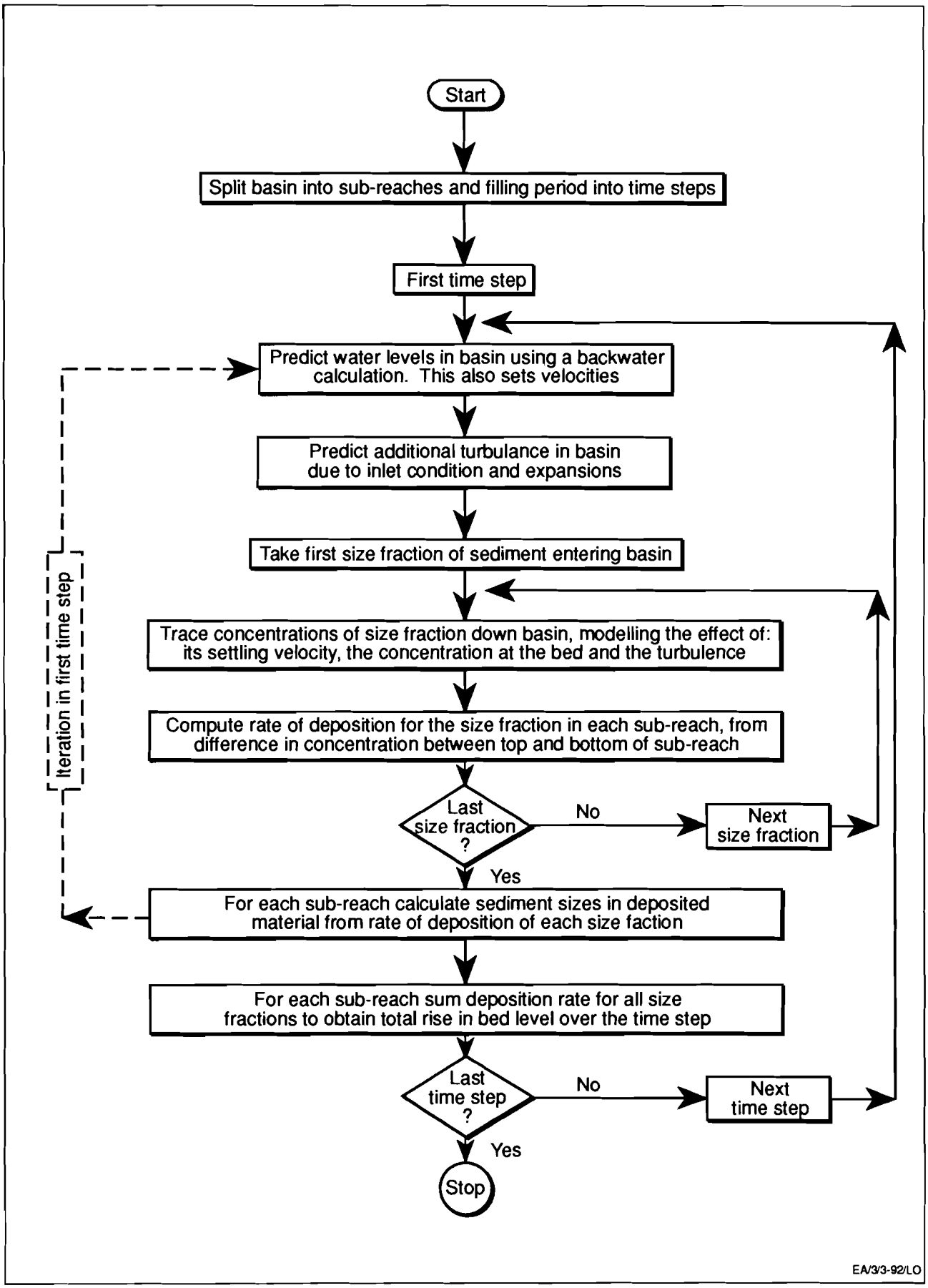

Figure 3 Flow chart showing overall structure of deposition model

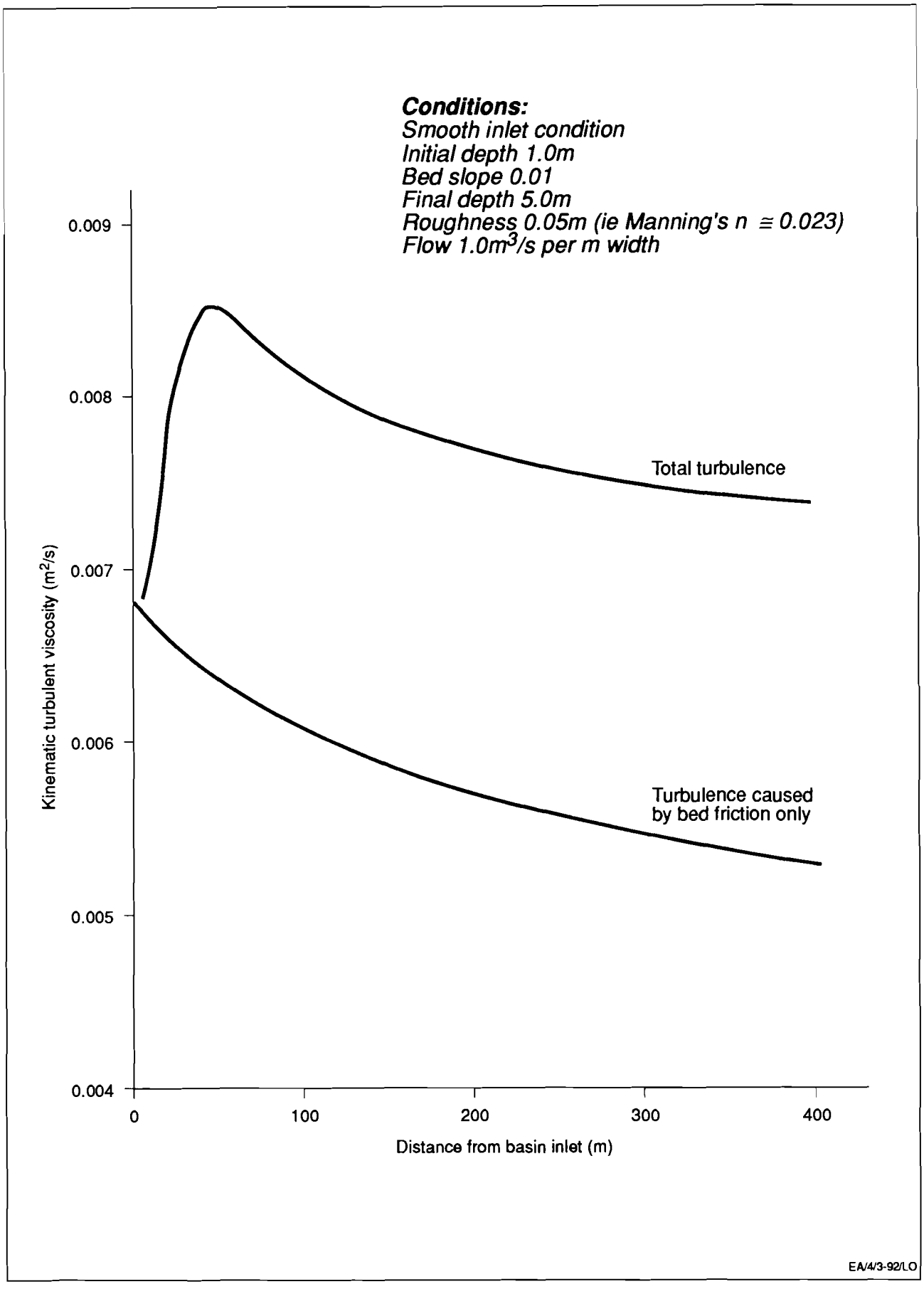

Figure 4 Turbulence in an empty basin with a continuously sloping bed

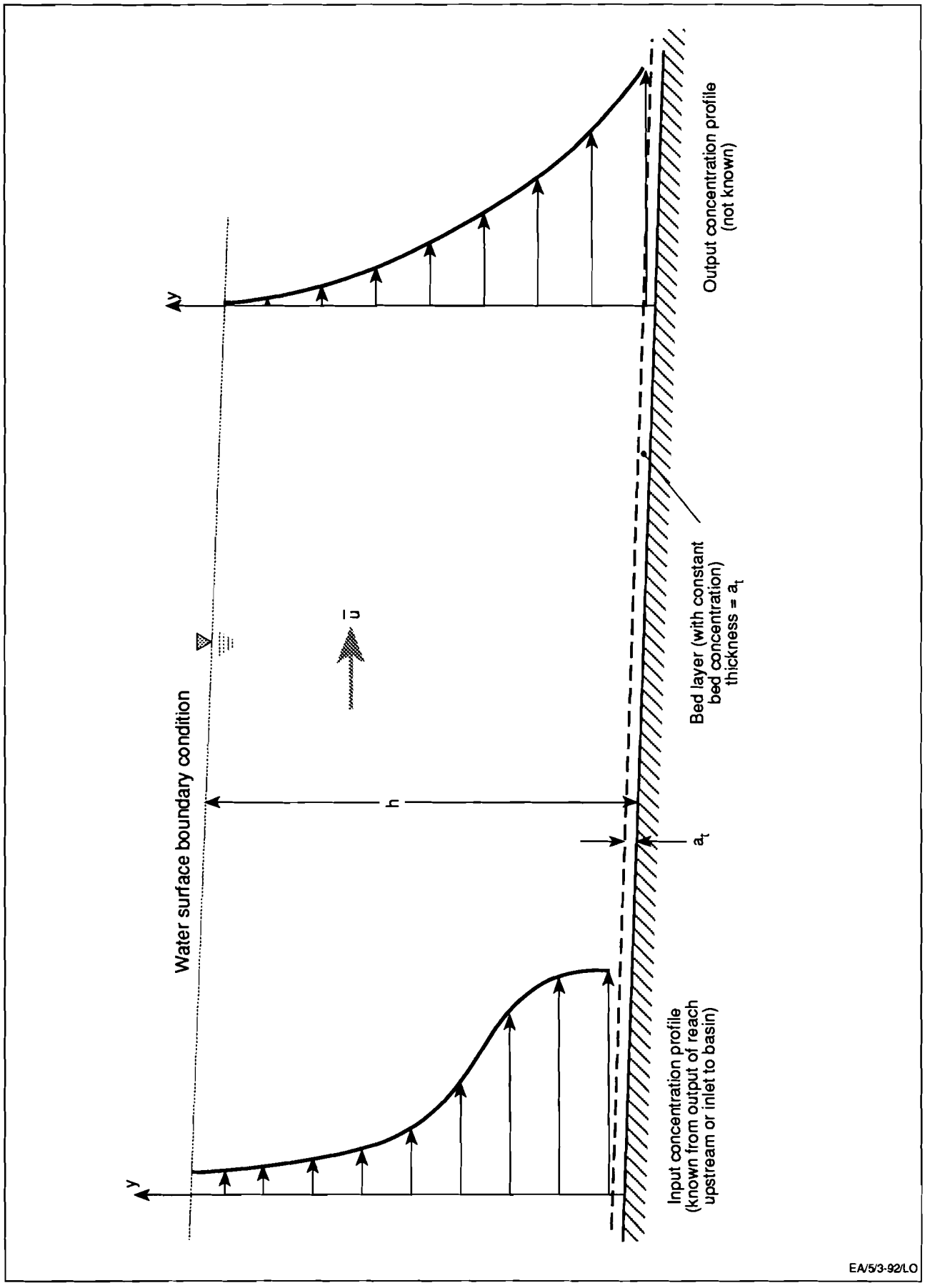

Figure 5 Sketch of turbulent diffusion problem within a sub-reach of the computational model

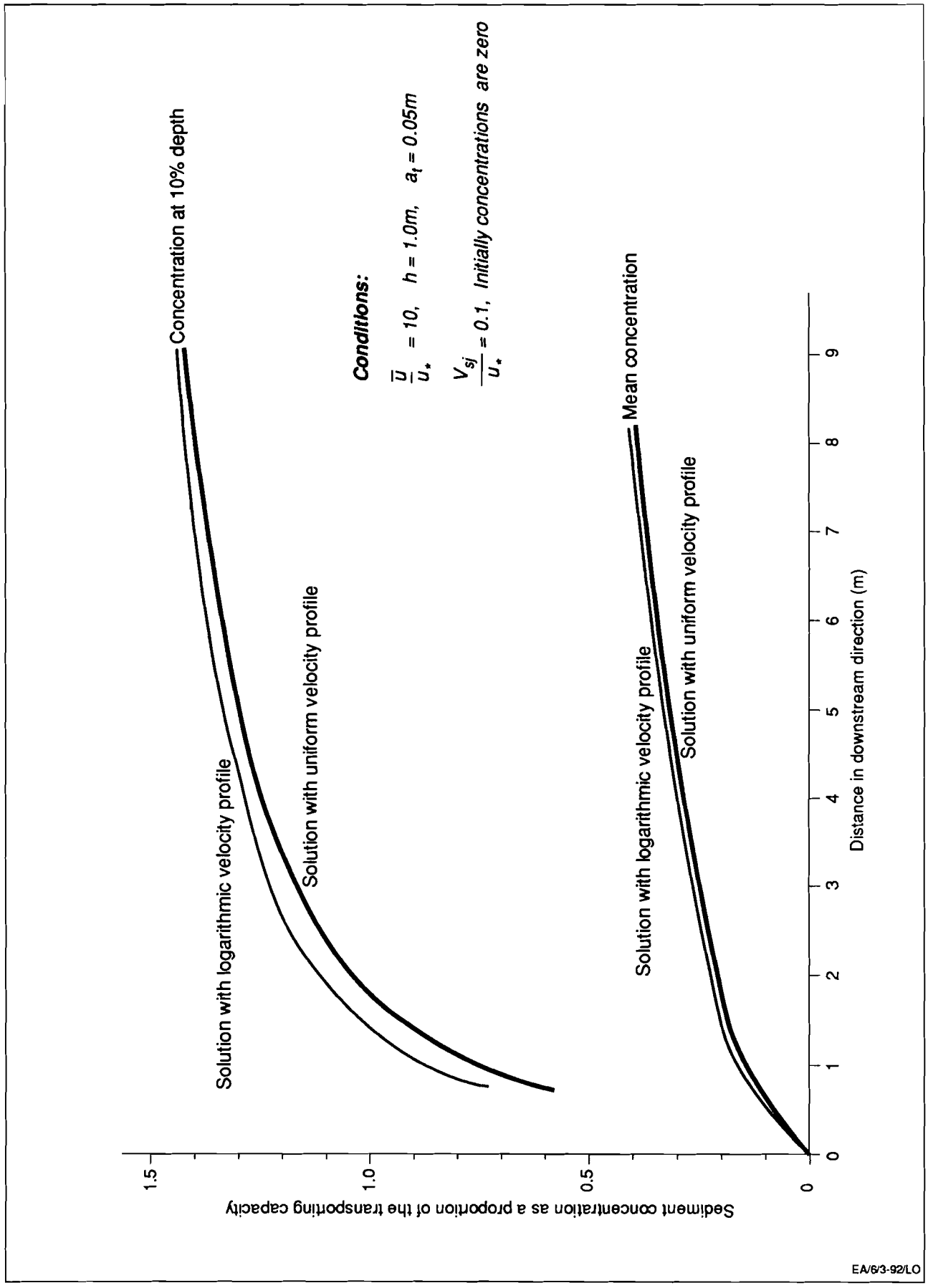

Figure 6 The effect of assuming a uniform velocity profile in the turbulent diffusion calculation

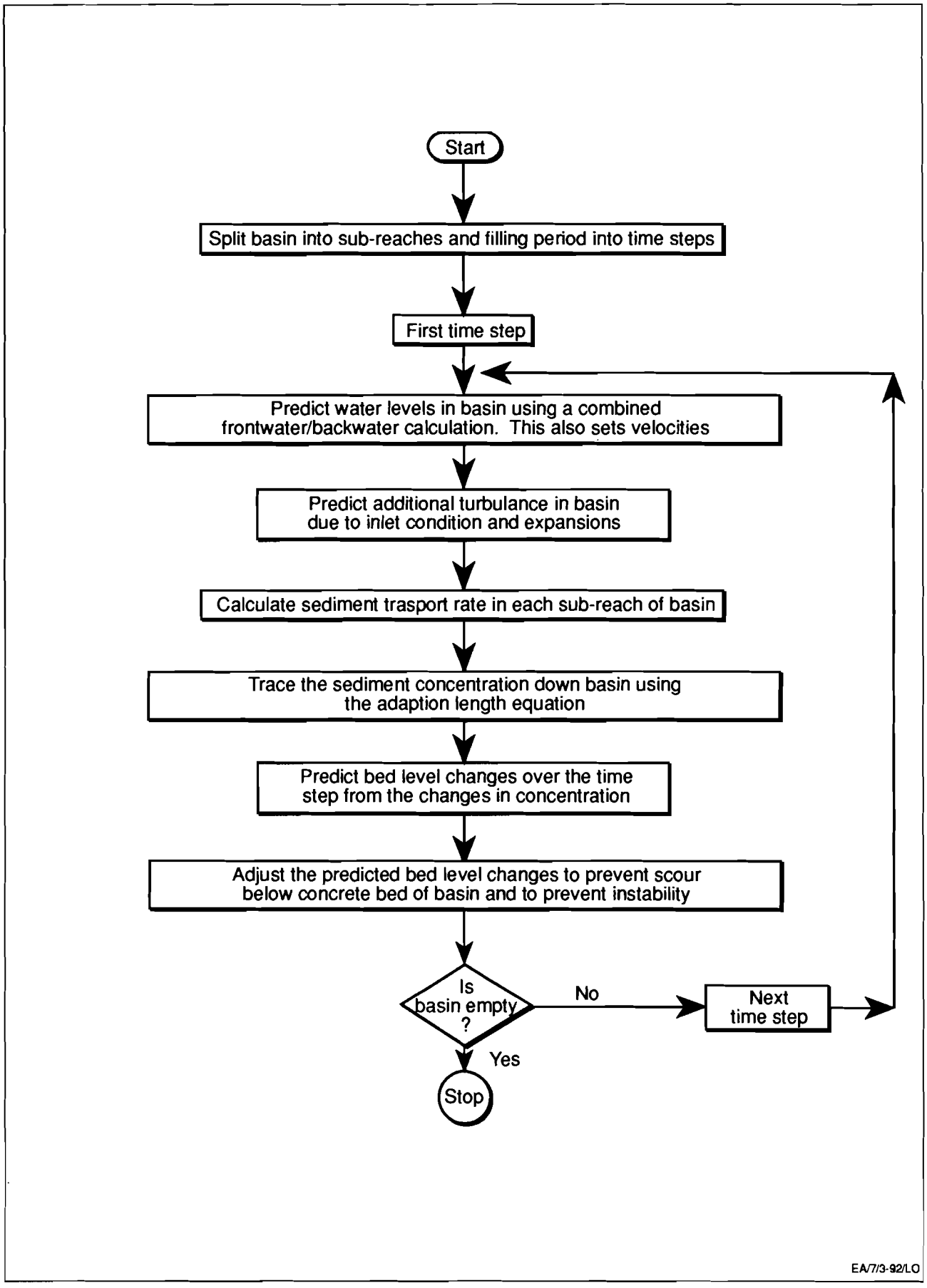

Figure 7 Flow chart showing overall structure of sluicing model

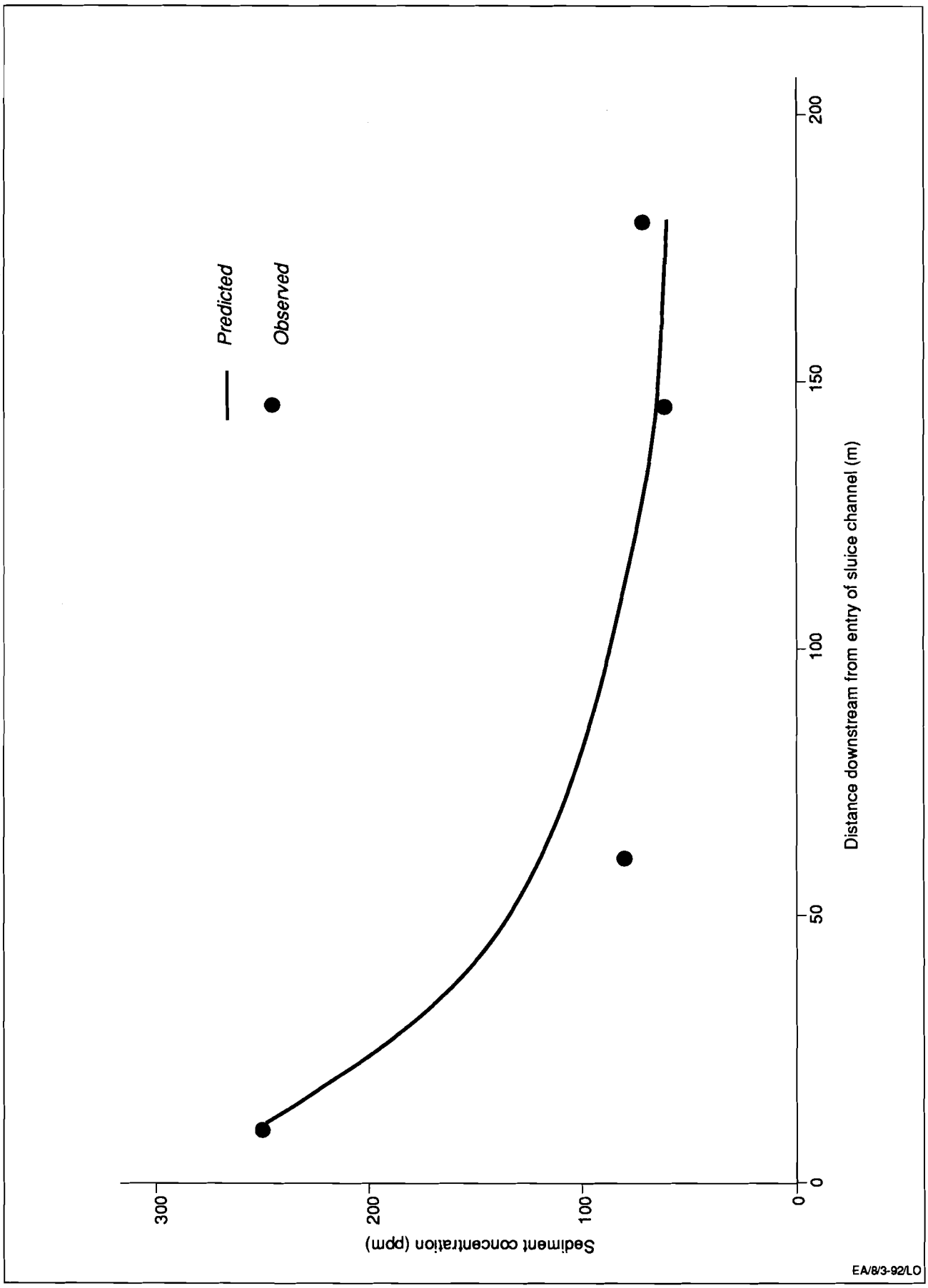

Figure 8 Comparison between predicted and observed deposition, Mae Tang sluice channel

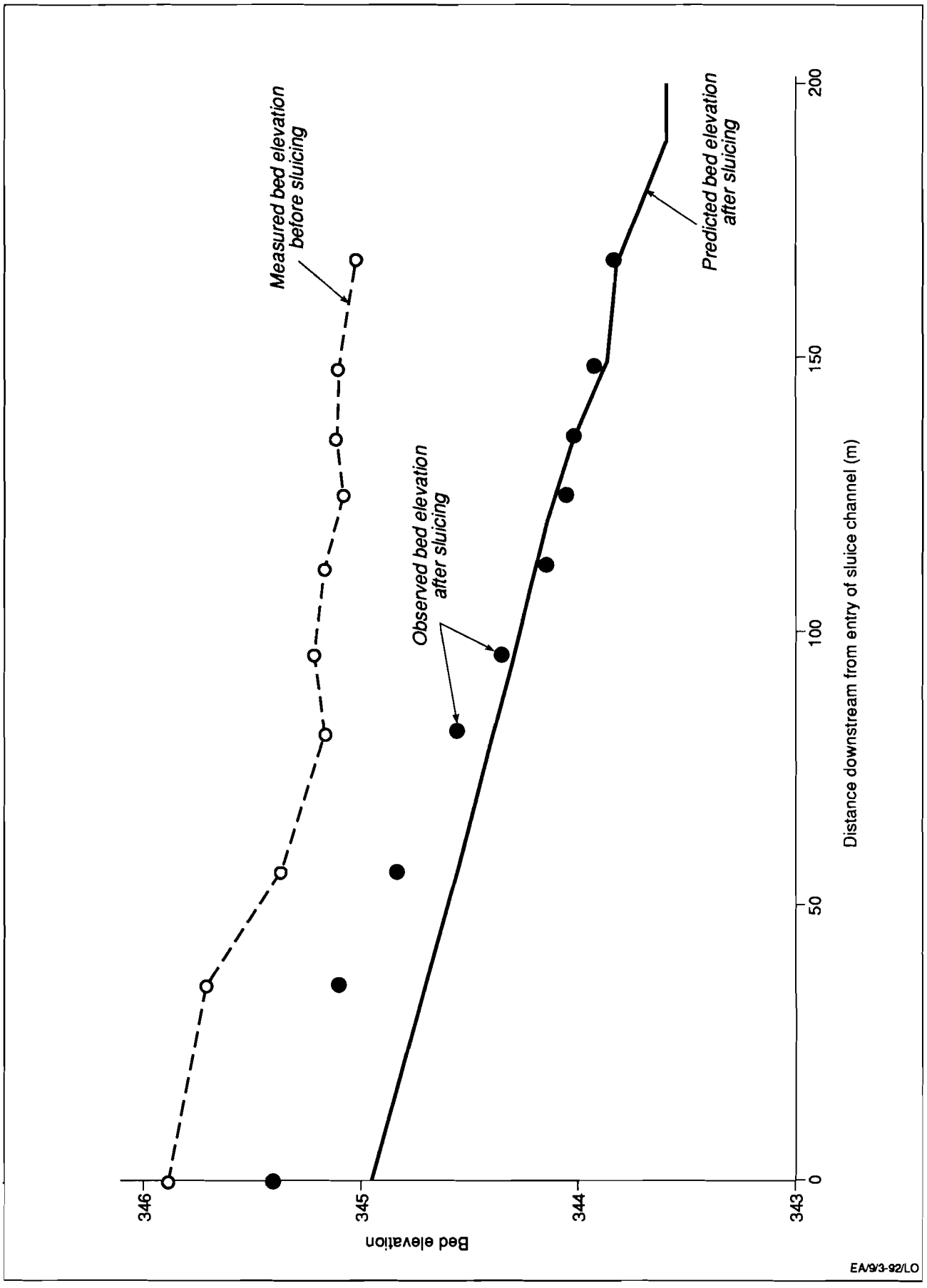

Figure 9 Predicted and observed bed elevations in the Mae Tang sluice channel

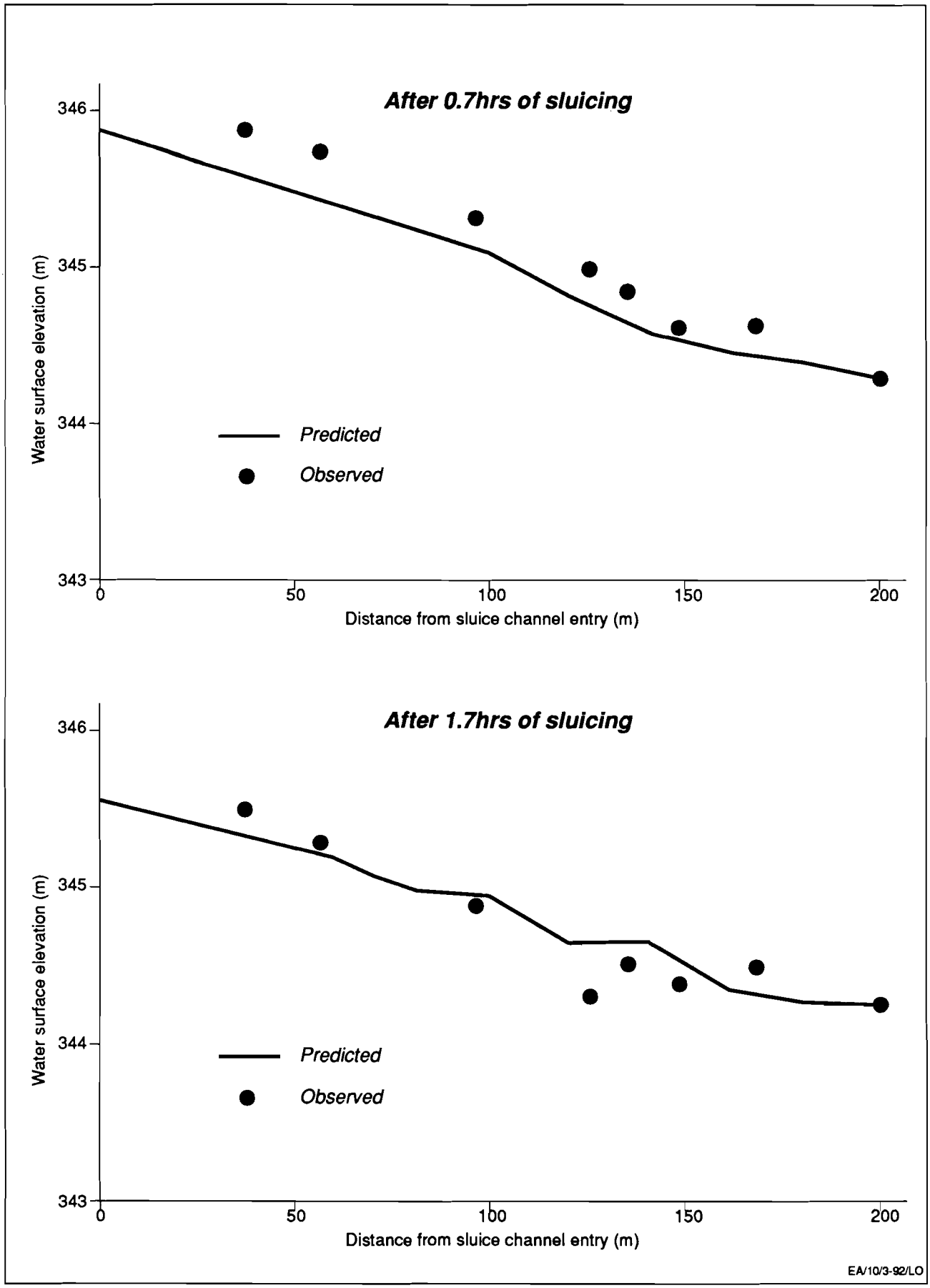

Figure 10 Predicted and observed water levels in the Mae Tang sluice channel during sluicing

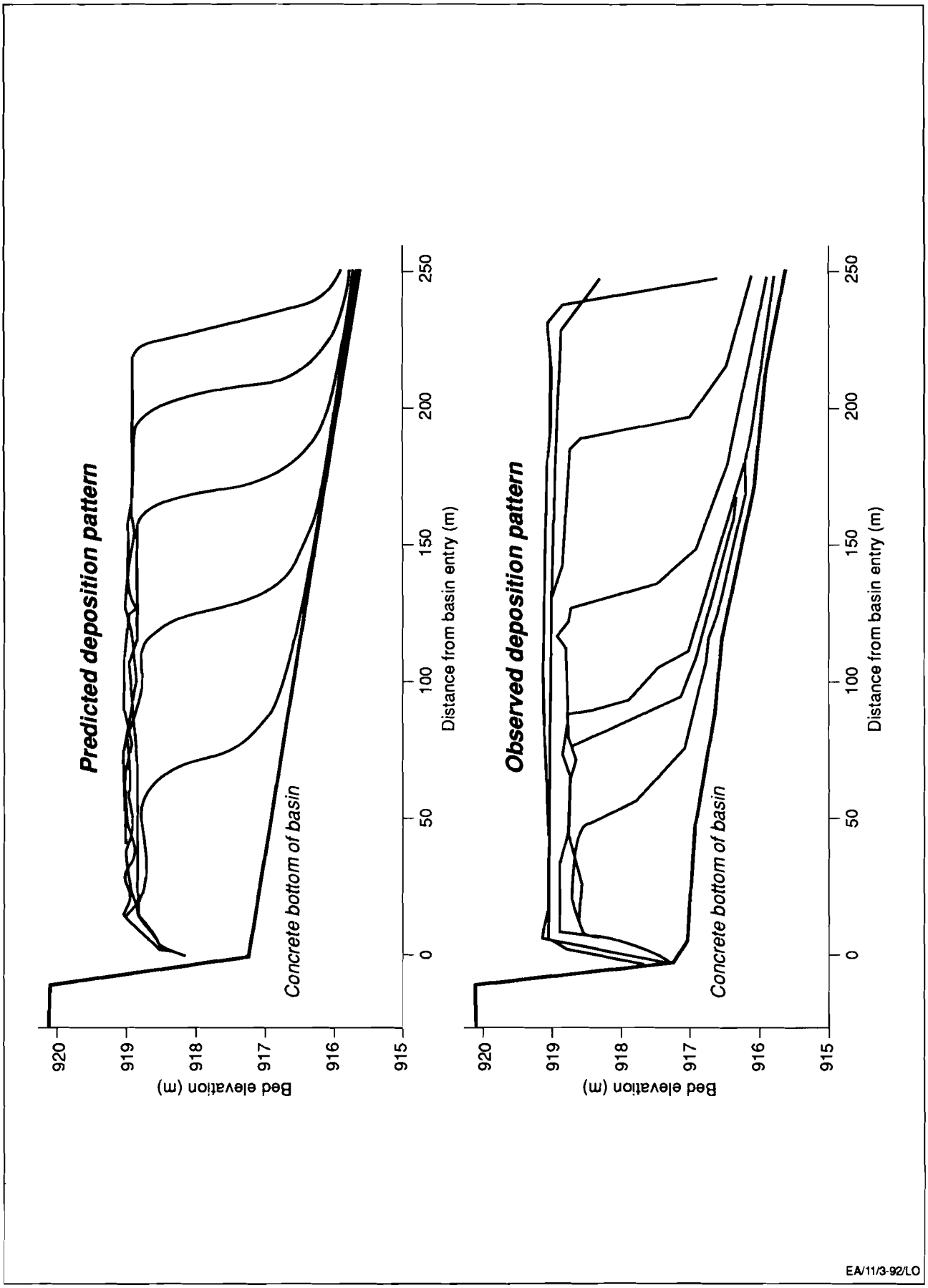

Figure 11 Comparison between predicted and observed deposition pattern, Yangwu settling basin. Silt deposition not simulated

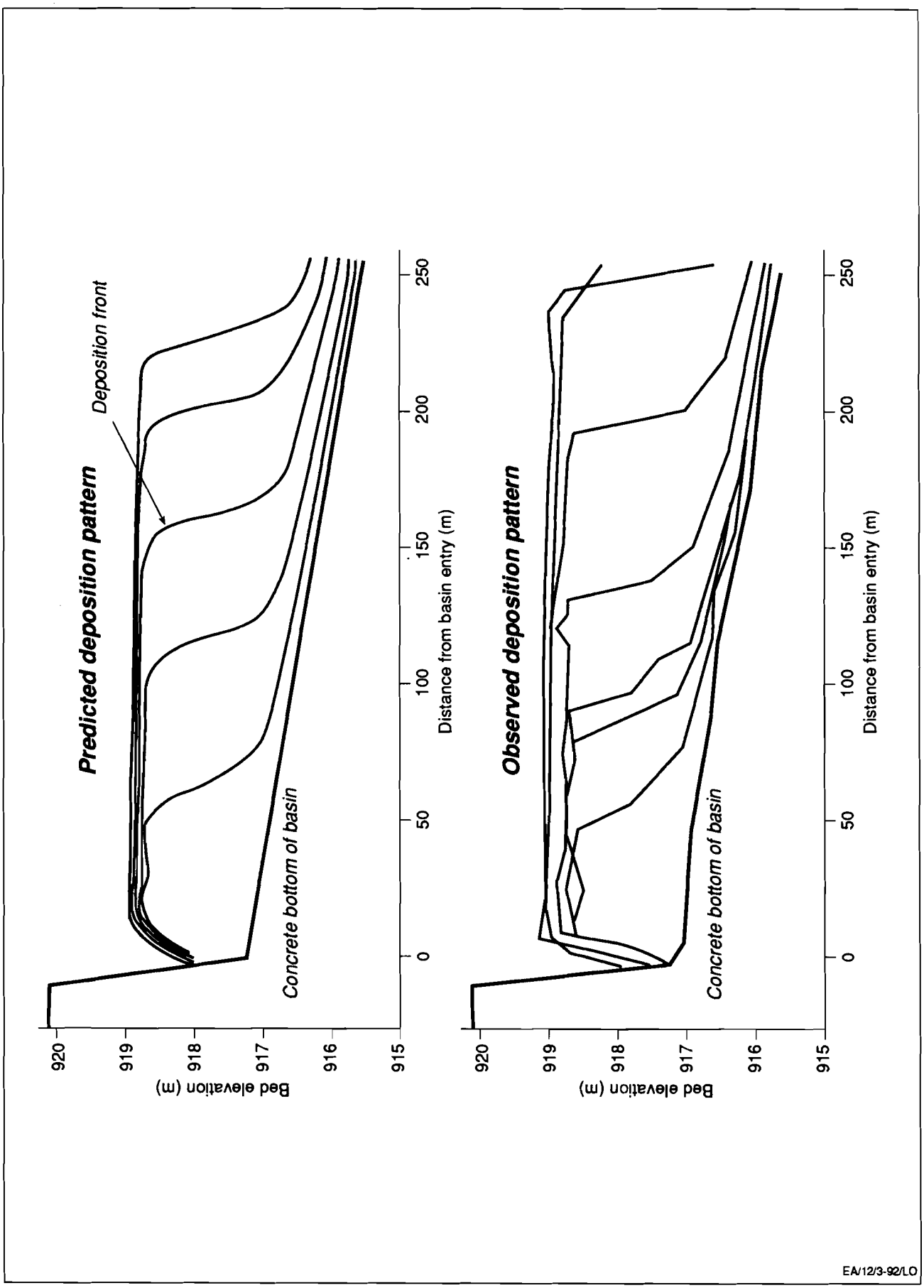

Figure 12 Comparison between predicted and observed deposition pattern, Yangwu settling basin. Simulation of silt deposition included

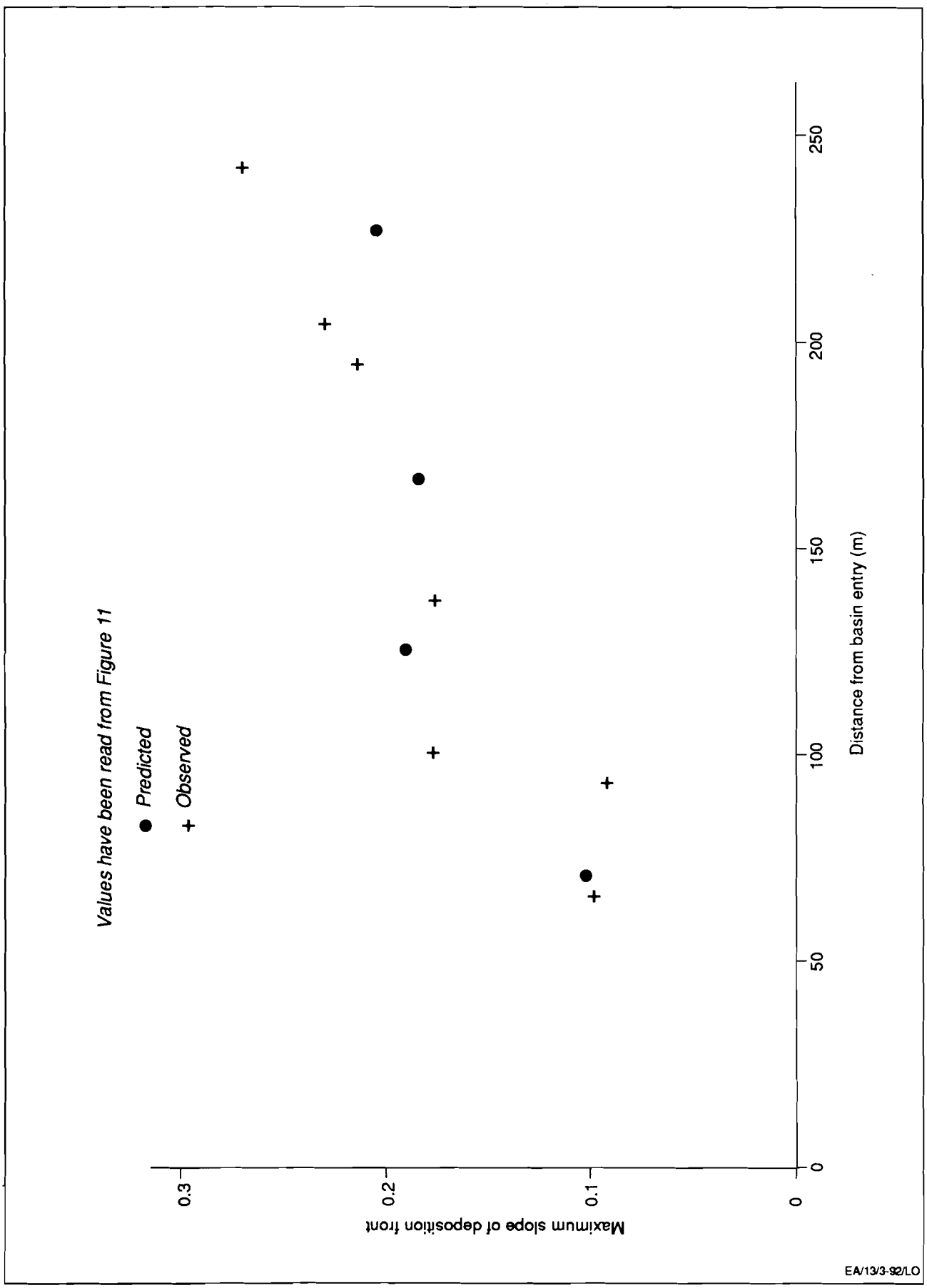

Figure 13 Predicted and observed slopes of the deposition front, Yangwu settling basin

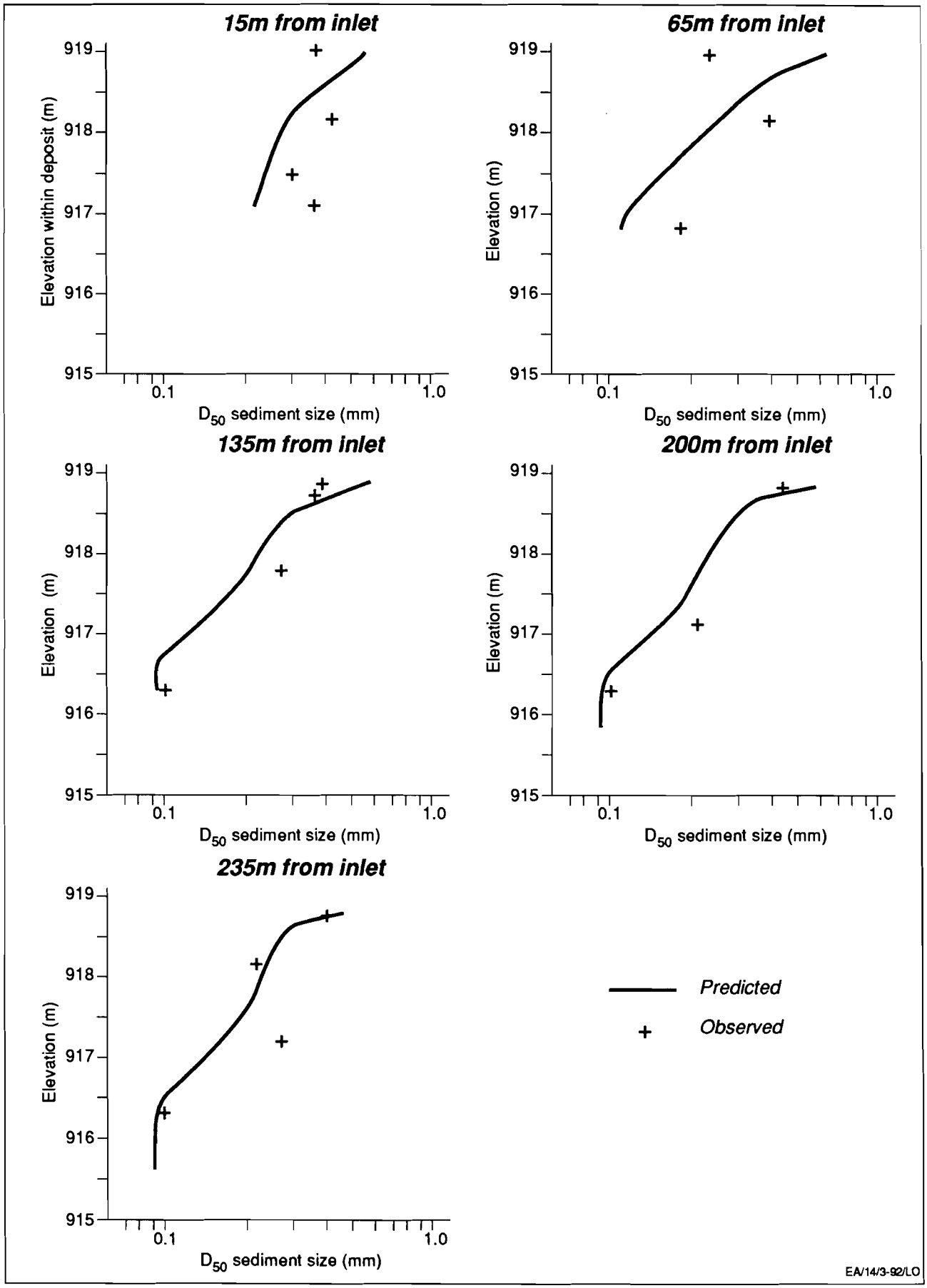

Figure 14 Predicted and observed sediment sizes in the Yangwu basin

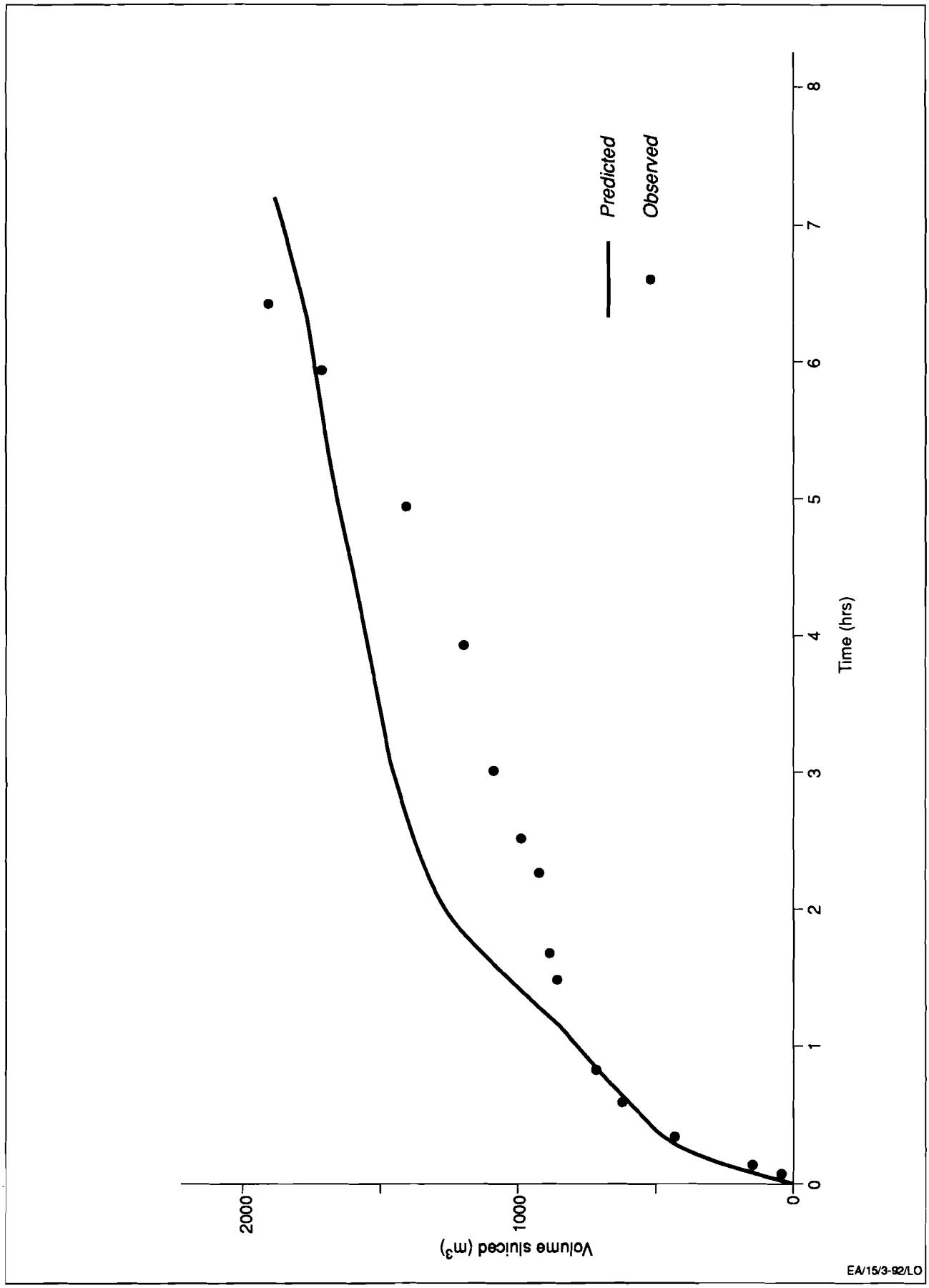

Figure 15 Predicted and observed sluicing rate, Yangwu basin

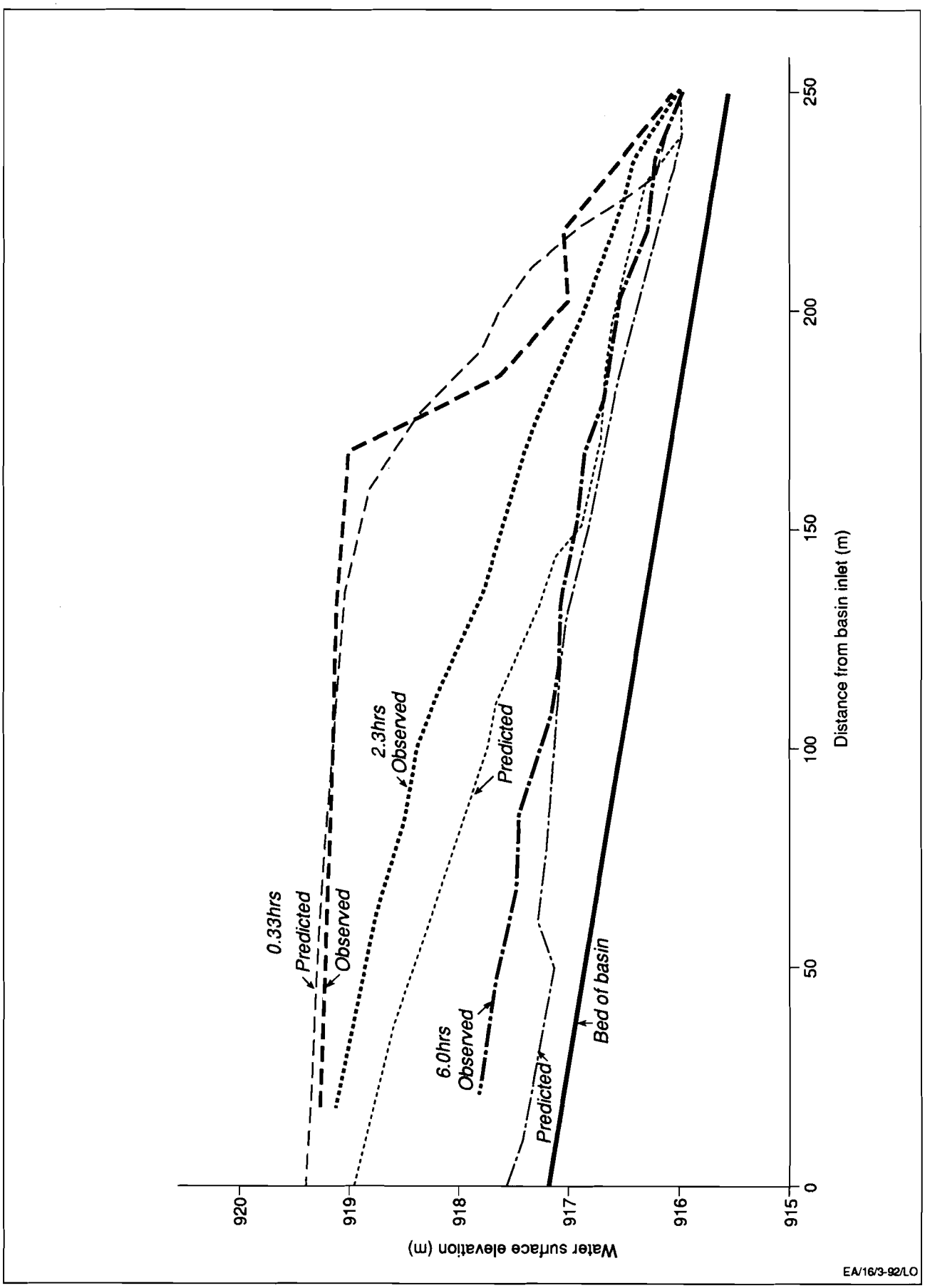

Figure 16 Comparison between predicted and observed water levels, Yangwu basin

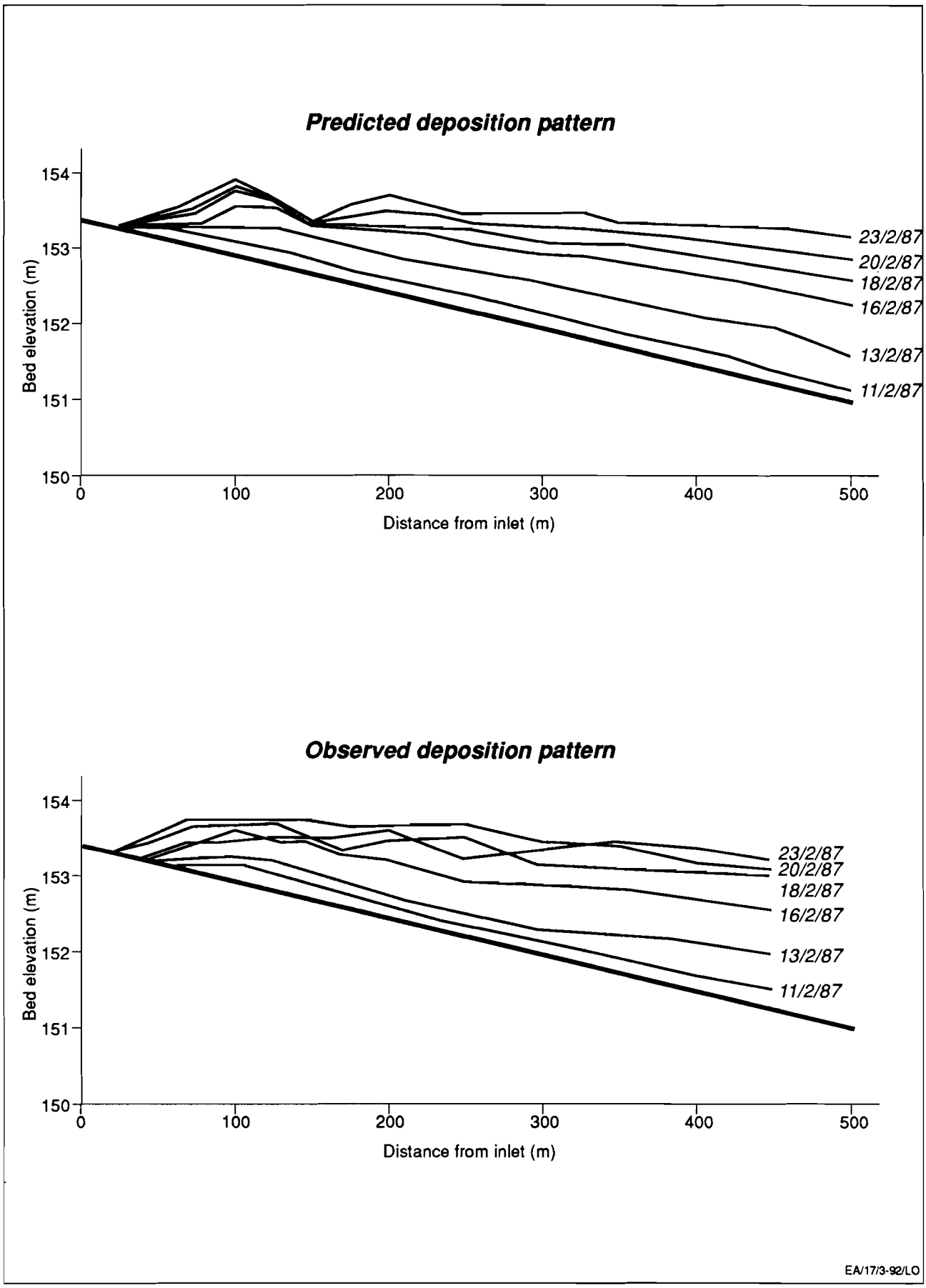

Figure 17 Comparison between predicted and observed deposition pattern, Karangtalun settling basin, 10-24 February filling period

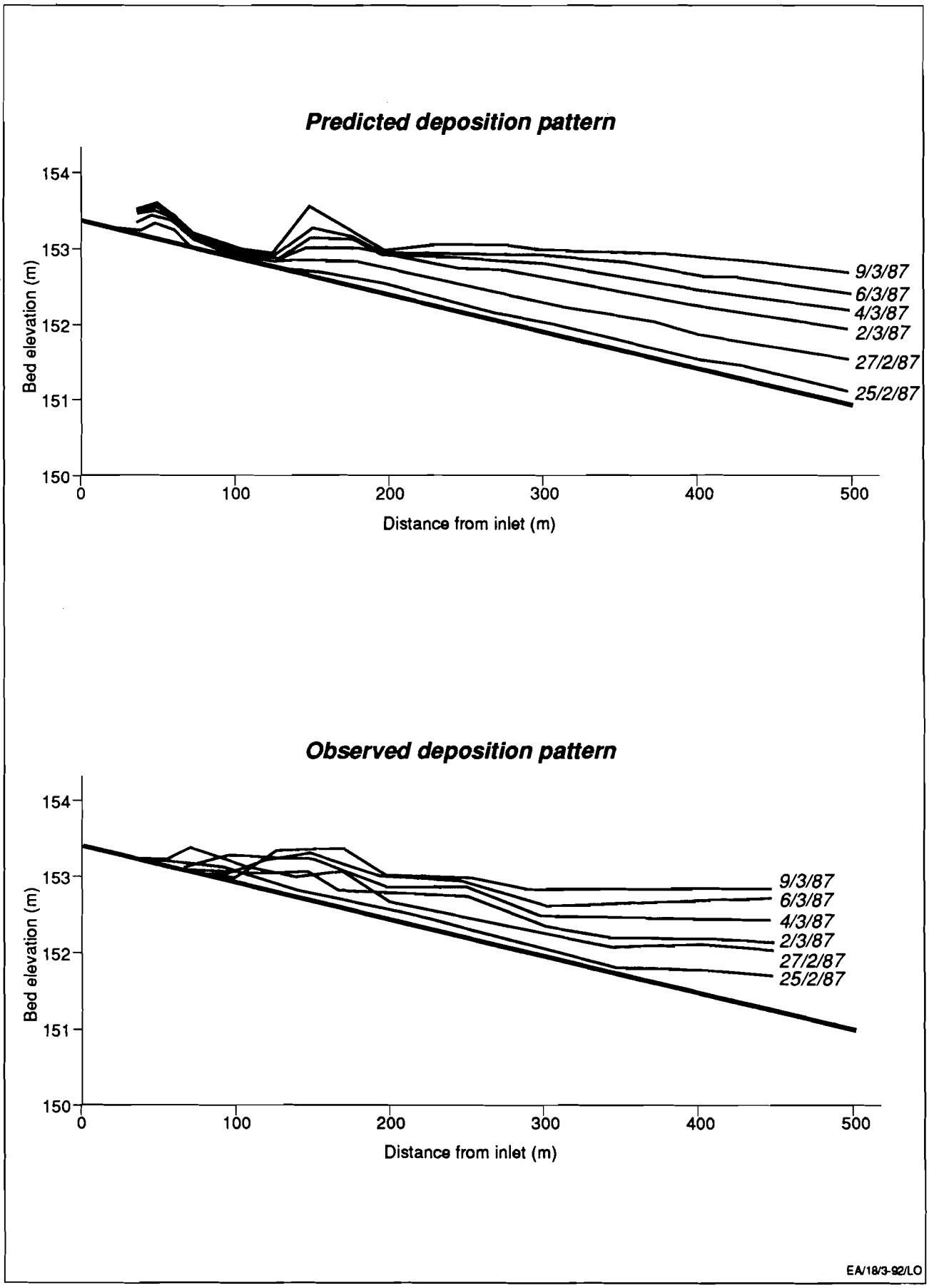

Figure 18 Comparison between predicted and observed deposition pattern, Karangtalun settling basin, 24 February-10 March filling period

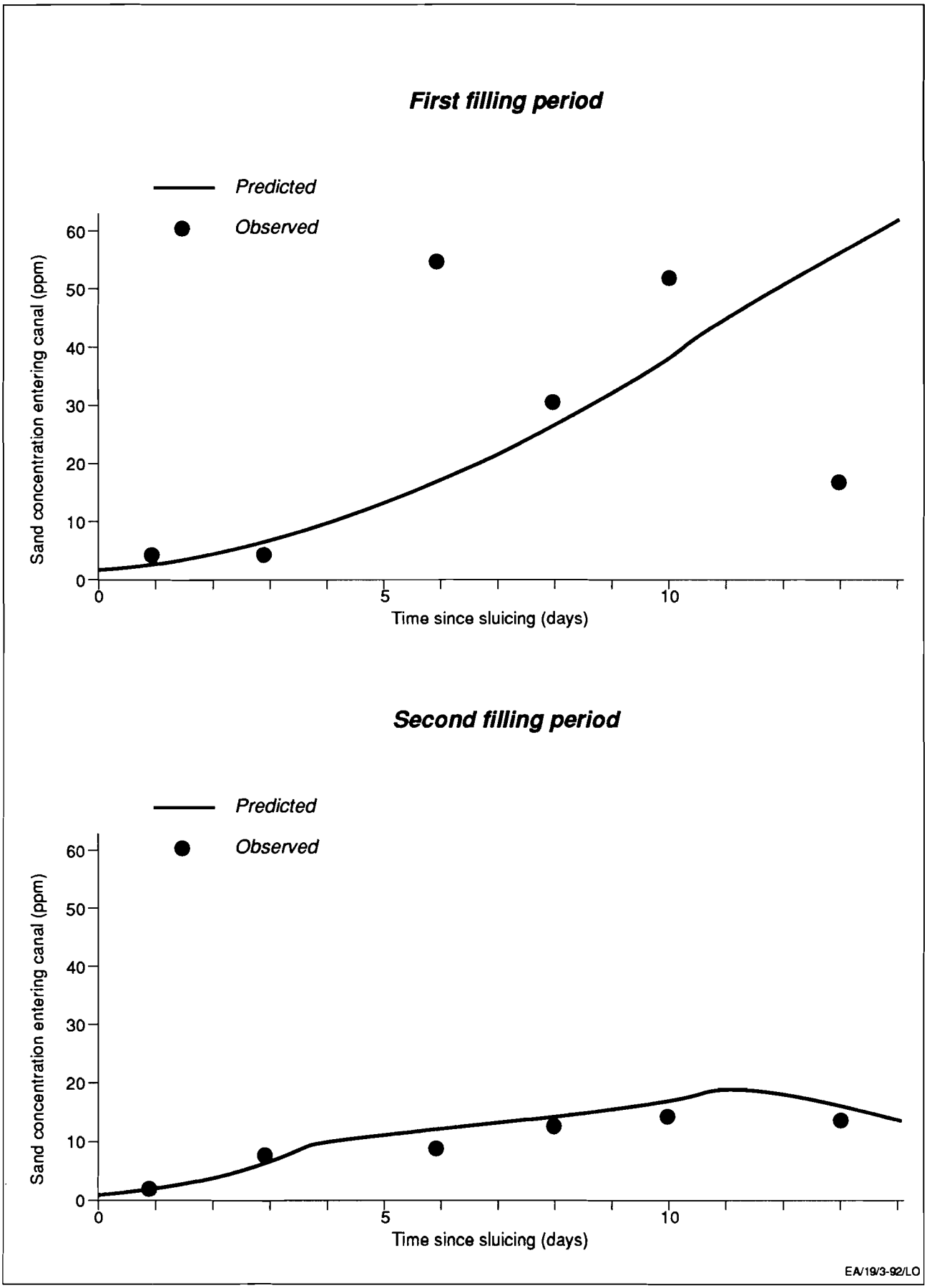

Figure 19 Predicted and observed sand concentrations entering canal, Karangtalun settling basin

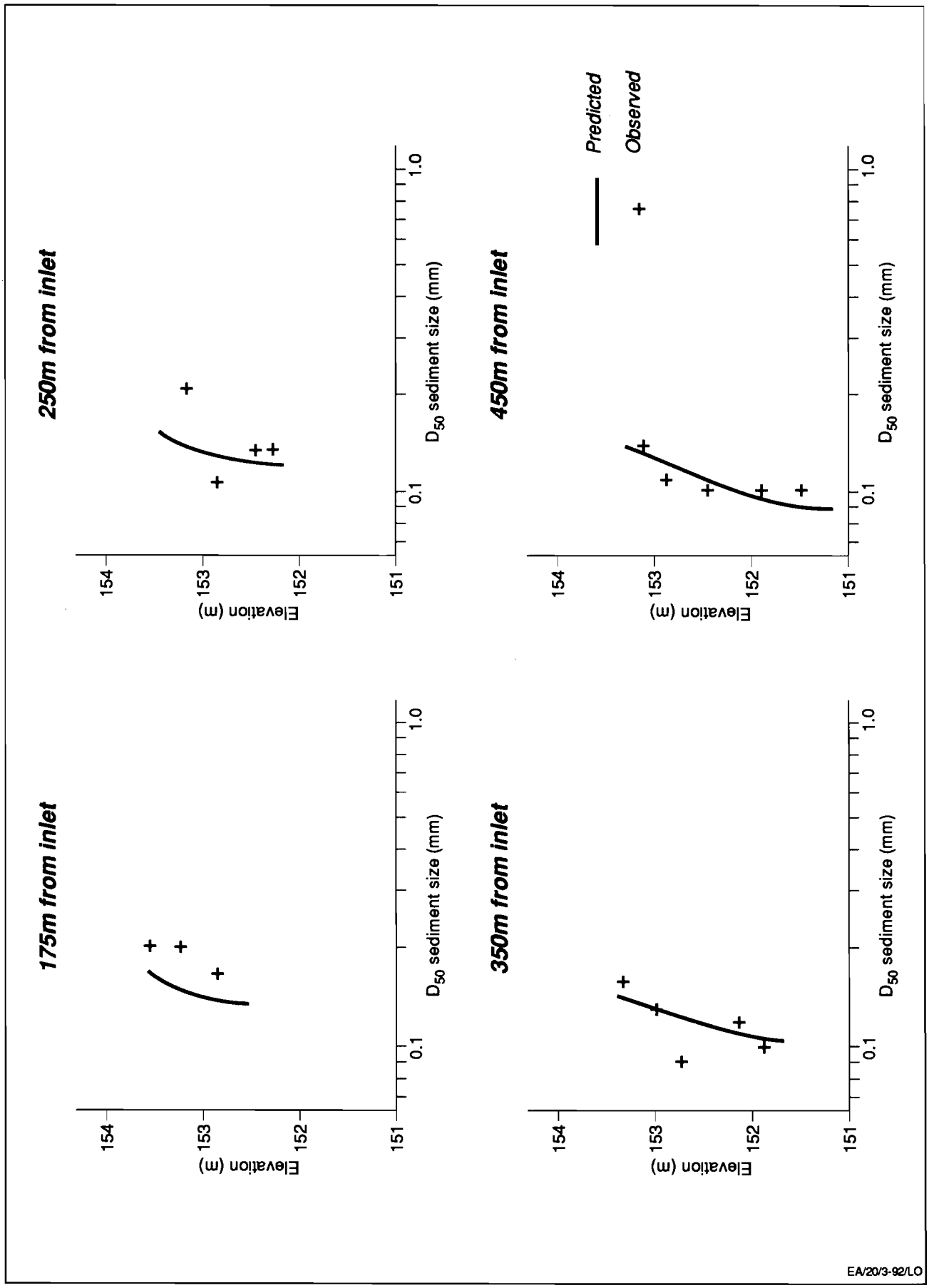

Figure 20 Predicted and observed sediment sizes in the Karangtalun basin, first filling period

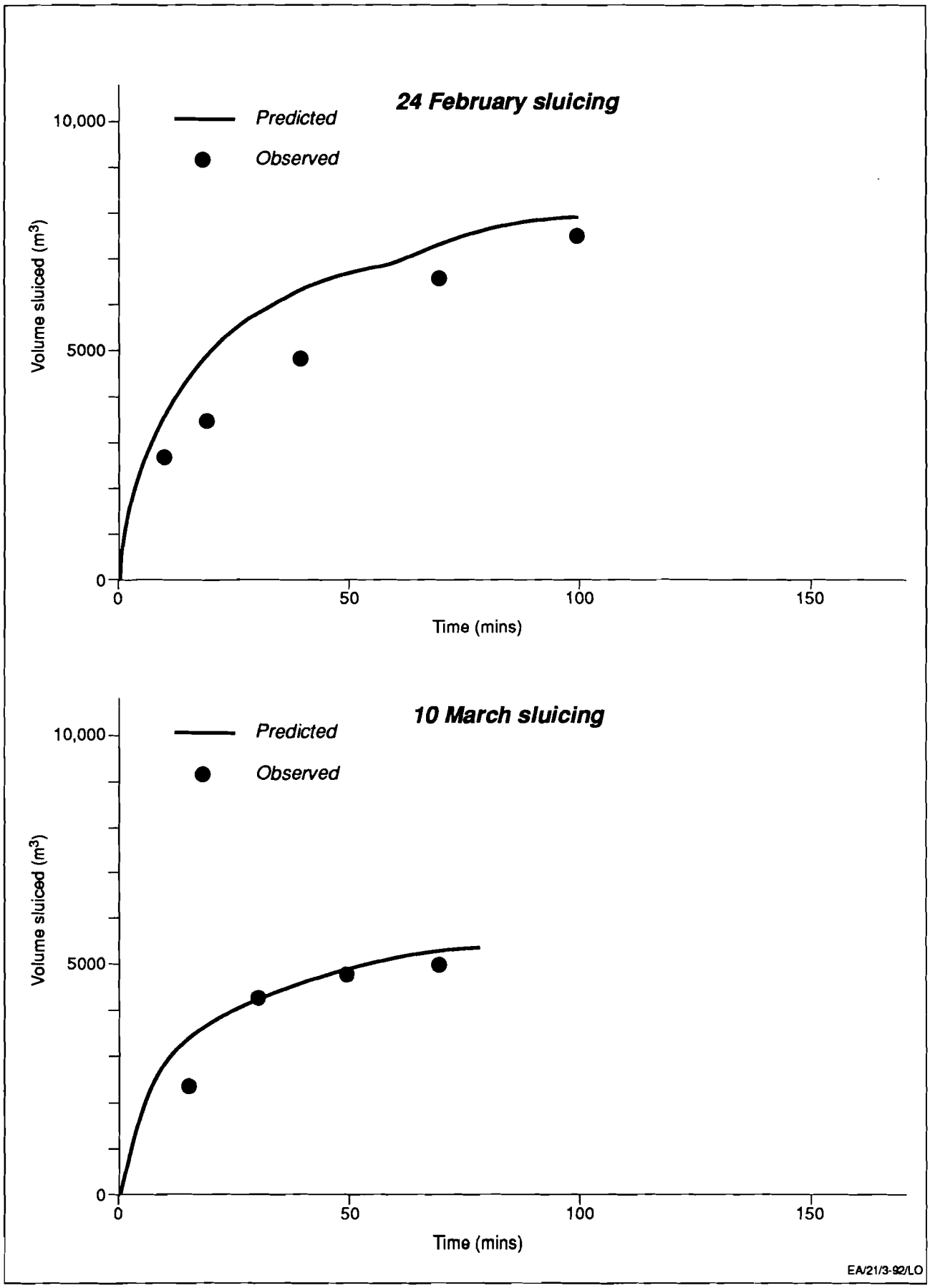

Figure 21 Predicted and observed sluicing rates, Karangtalun basin

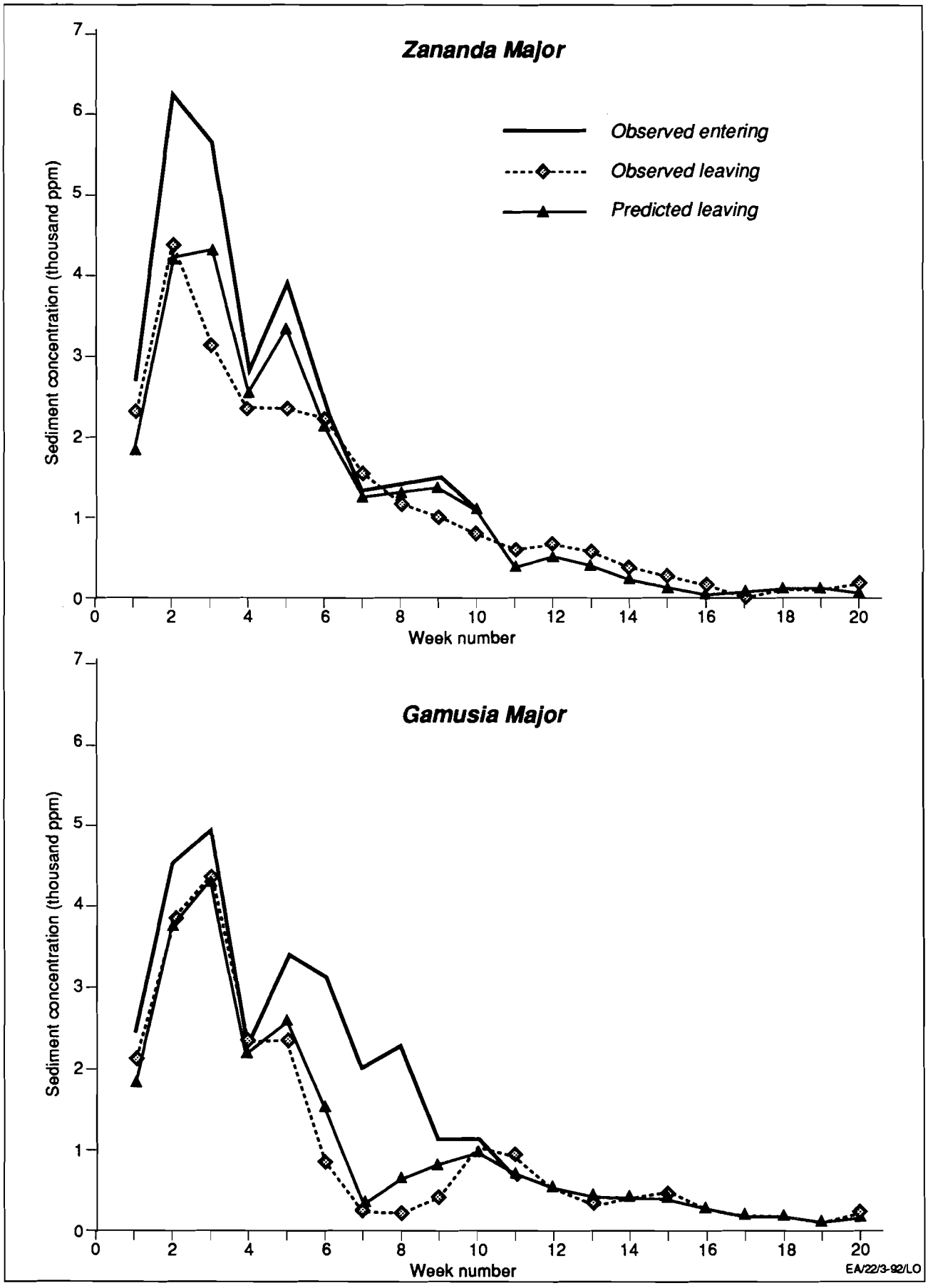

Figure 22 Predicted and observed sediment concentrations in the first reach of Zananda Major and Gamusia Major

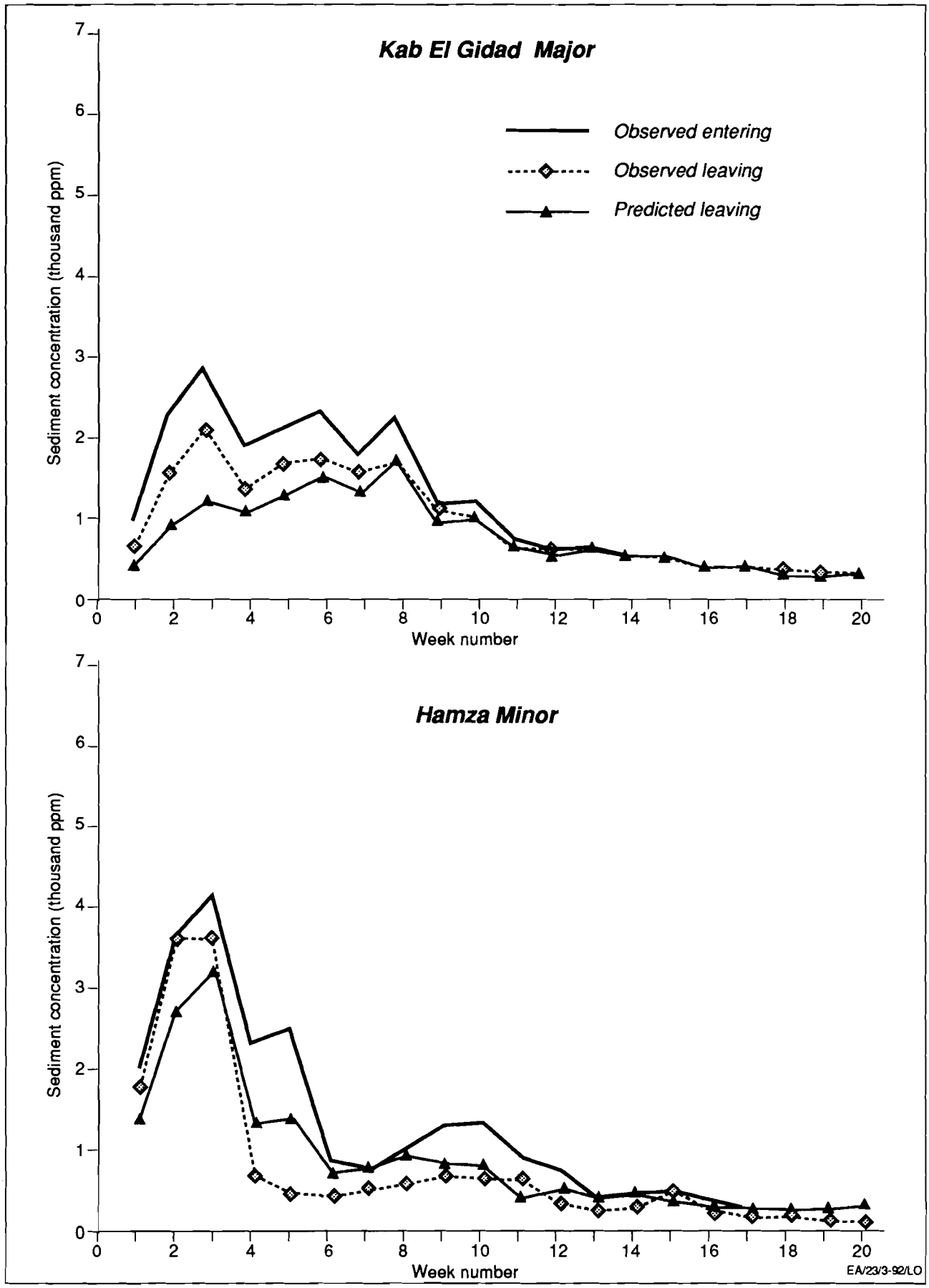

Figure 23 Predicted and observed sediment concentrations in the first reach of Kab El Gidad Major and Hamza Minor

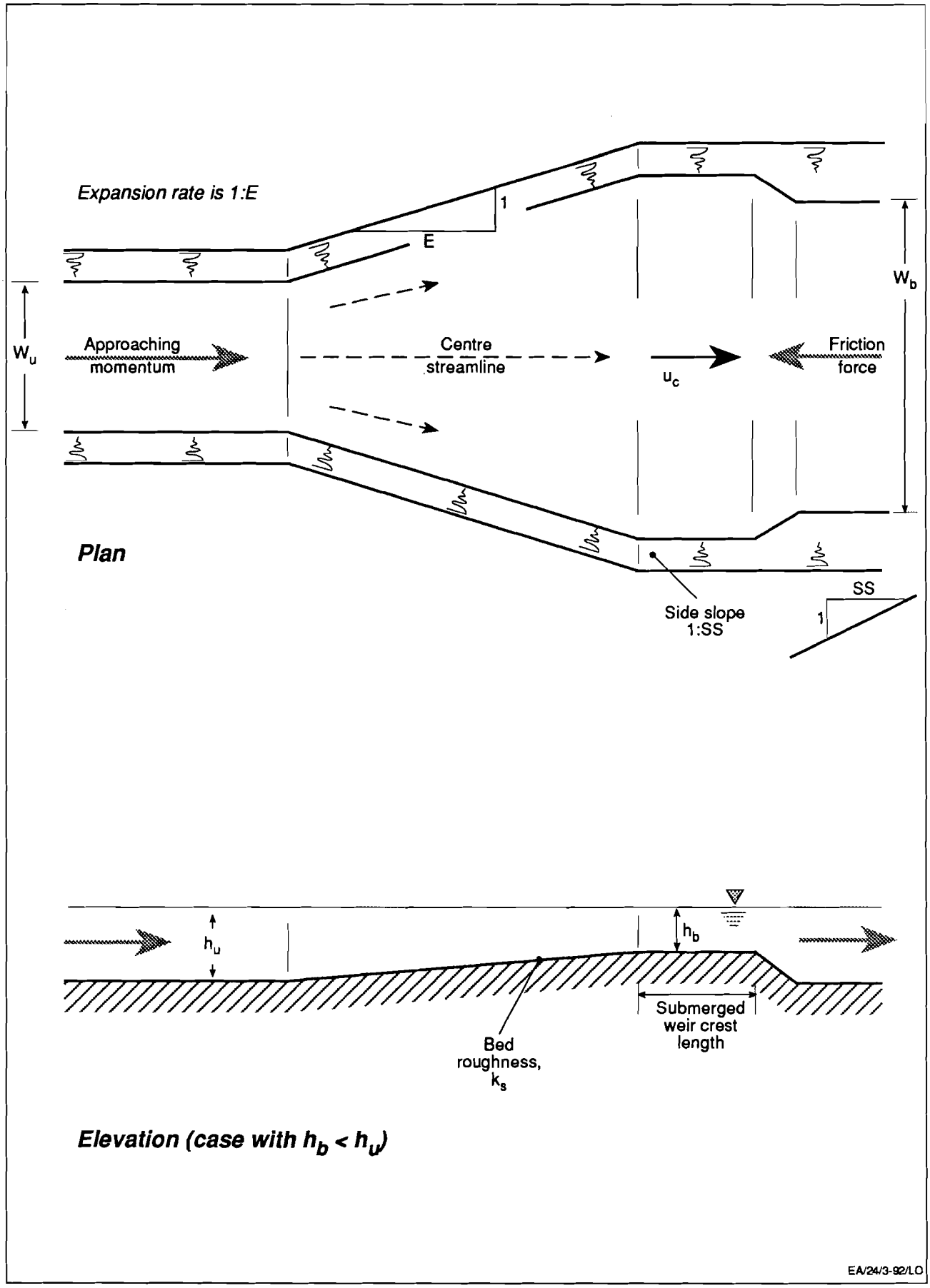

Figure 24 Plan and elevation of an entry section to a settling basin

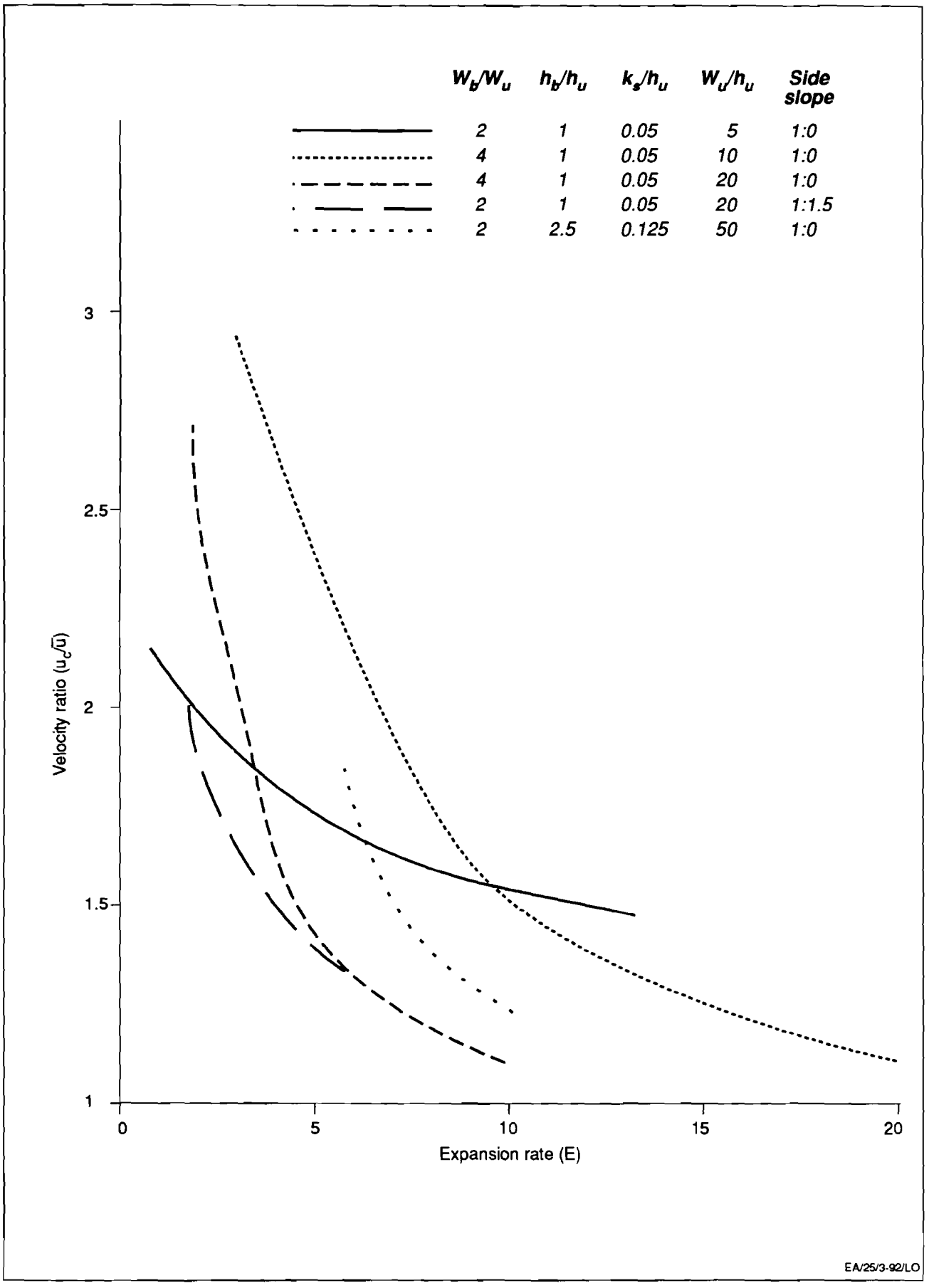

Figure 25 Velocity ratio as a function of expansion rate

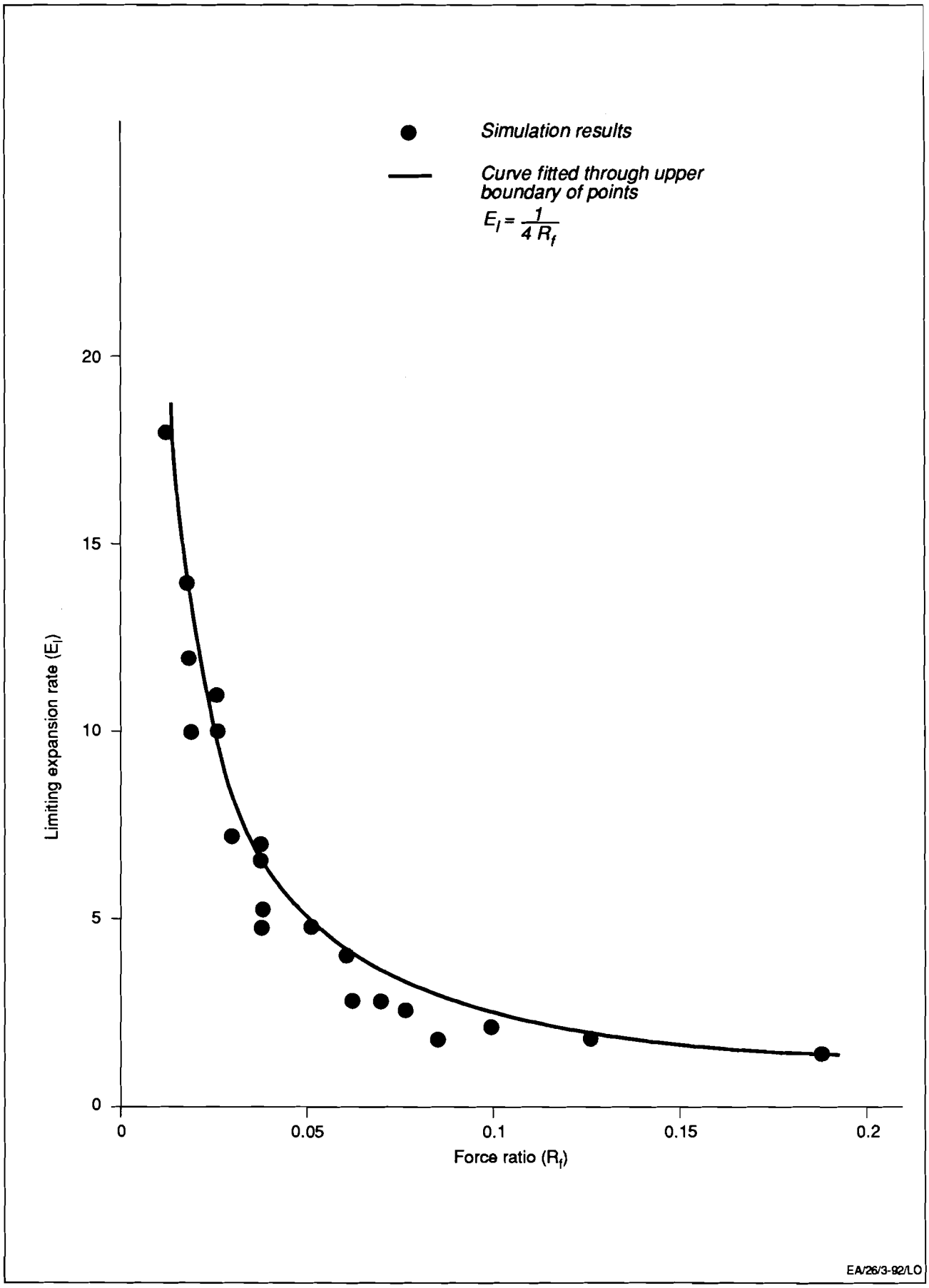

Figure 26 Relationship between limiting expansion rate and force ratio

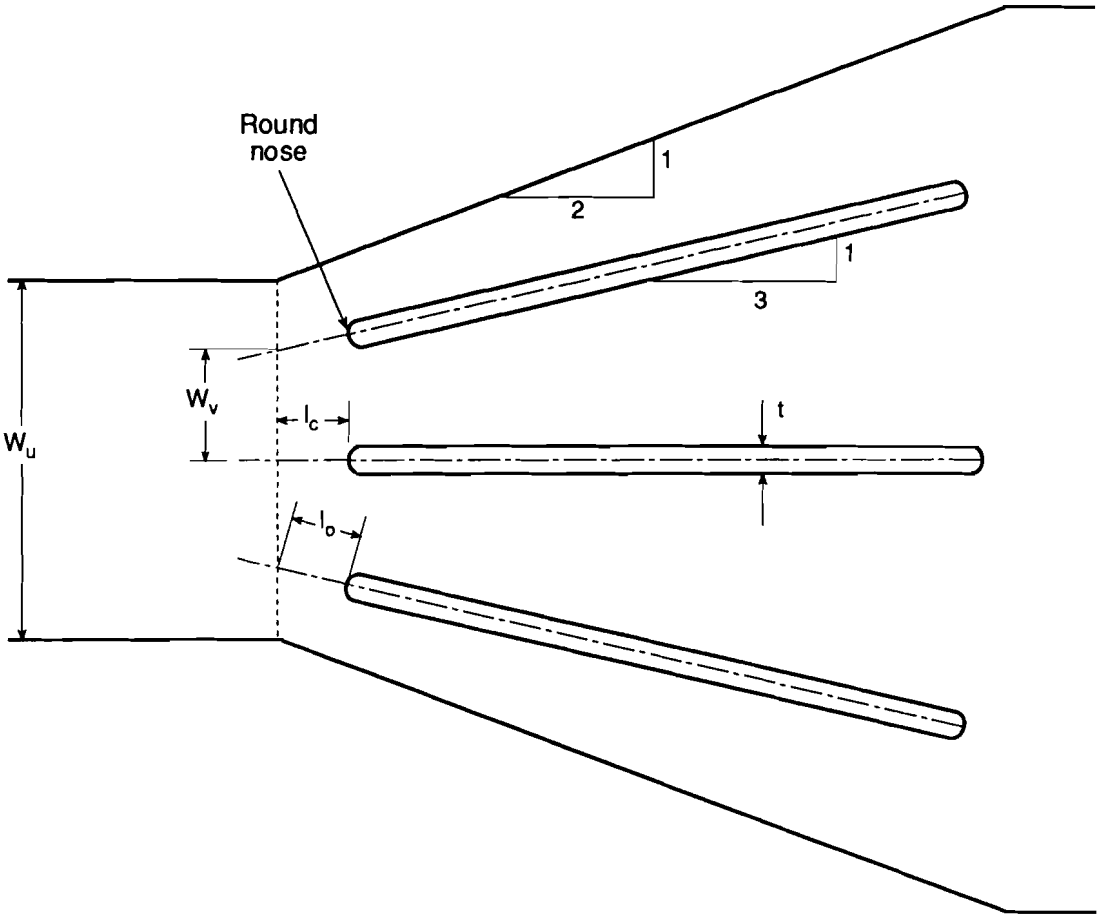

$W_v = 0.3\ W_u$

$l_o = 0.15\ W_u$

$l_c = 0.15\ W_u$

$t \leq 0.06\ W_u$

EA/27/3-92/LO

Figure 27 Recommended geometry for vanes at a basin entry

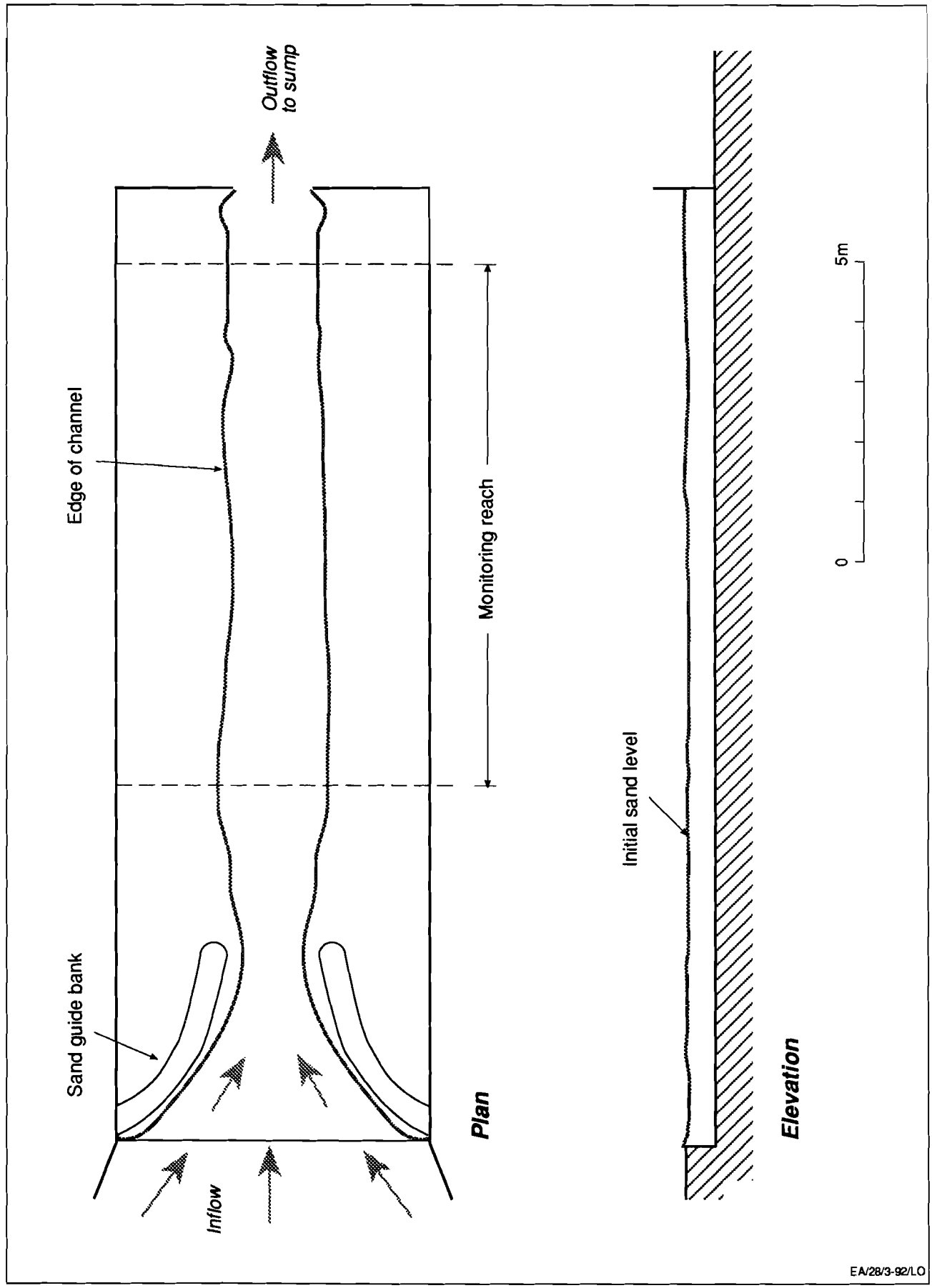

Figure 28 Basin layout for sluicing width tests

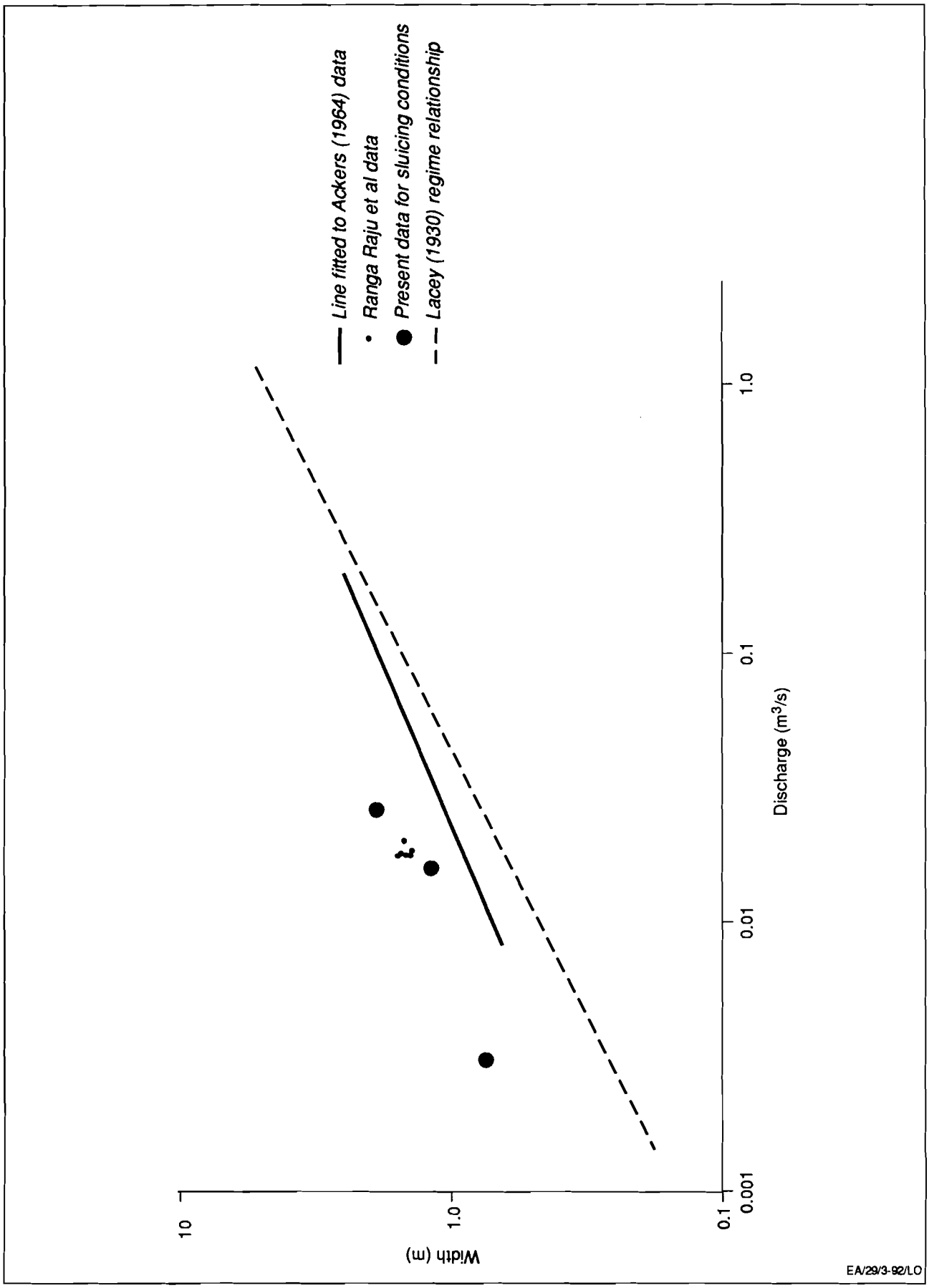

Figure 29 Relationships between channel width and discharge

Appendix

Appendix: Outline Design Procedure for Sluiced Settling Basins

A design procedure is given in summary in Figure A1, it is set out in more detail below.

I) Data Requirement

The data requied by the procedure includes

a) The target sediment concentrations passing the basin for the sands and for silts and clay, together with data on the concentrations entering the basin.

b) Sediment sizes or settling velocities and their specific gravity.

c) Densities of deposited material.

d) Basin discharges and the required water surface elevations at the downstream end of the basin during normal operation and during sluicing.

II) Setting an Initial Basin Layout

a) Use Vetter's equation to derive a first estimate for the basin plan area.

b) Use the work of Section 4 to set the basin width, this sets the length.

c) Set the initial bed elevation at the downstream end of the basin from water surface elevation during sluicing, and set the bed elevation at the upstream end of the basin as equal to the elevation in the channel upstream.

d) Select a side slope for the basin.

III) Modify Basin Design Using the Numerical Models

a) Run the deposition model.

b) Make the following adjustments to the design in the light of the model predictions, as appropriate.

i) If either the sand or the silt/clay concentrations passing the basin are too high then the basin should be made larger.

ii) If the time taken for the basin to fill is too short then its storage should be increased.

iii) If the concentrations leaving the basin are low for much longer than a minimum filling time, then there is scope for making the basin smaller.

c) If design changes are made then run the deposition model again for the new geometry.

d) Run the sluicing model.

e) Make further changes to the basin design in the light of the sluicing model predictions.

i) If the time to sluice the basin is too long then a range of options can be tried:

- The basin can be made shorter.
- The difference in elevation between the sluicing and normal operation water levels can be increased.
- The sluicing discharge can be set greater.
- A twin basin can be considered.

ii) If the sluicing time is very short then the basin's storage can be increased.

f) If changes to the basin are required then both the deposition model and the sluicing model must be run again.

g) Continue model runs and design modifications until a suitable design has evolved.

IV) Other Aspects of Design

a) Set the design details of the entry to the basin using the recommendations of Section 4.1.

b) Re-check for scour in the downstream canal system.

c) Design the escape channel from the basin to the sediment disposal point, if it is required.

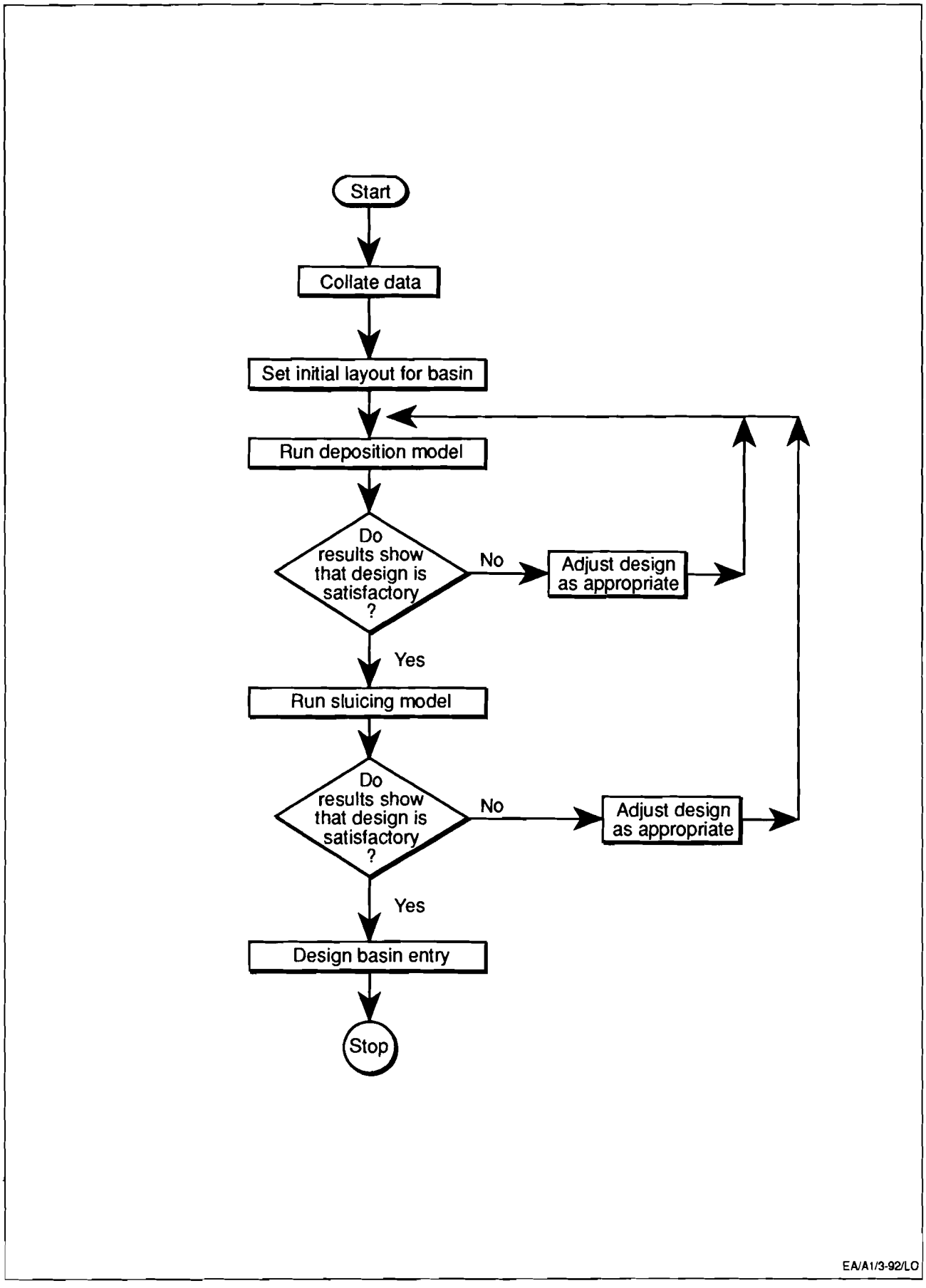

Figure A1 Summary of settling basin design procedure

This report is one of a series on topics of water resources and irrigation, prepared by HR Wallingford and funded by the British Overseas Development Administration

Others in the series include :

OD 111	Dallao soil erosion study, Magat catchment, The Philippines – Summary report (1984-87). (In collaboration with the National Irrigation Administration, Government of The Philippines)	M B Amphlett & A Dickinson
OD 112	Hakwatuna Oya water management study, Sri Lanka: Assessment of historical data and performance in Maha 1988/89 season	J D Bird & M Y Zainudeen
OD 113	Water management at Kraseio irrigation project – Analysis of historical data	J C Skutsch & H Goldsmith
OD 114	Socio-economic parameters in designing small irrigation schemes for small scale farmers: Nyanyadzi case study. Report I: The effect of drought on water distribution and farm incomes on the Nyanyadzi irrigation scheme, Zimbabwe	M Tiffen, C Harland & C Toulmin
OD 115	Report II: Net agricultural incomes and plot sizes	M Tiffen & M Glaser
OD 116	Report III: Managing water and group activities; implications for scheme design and organisation	M Tiffen
OD 117	Report IV: Summary and conclusions	M Tiffen
OD 118	Workshop on sediment measurement & control and design of irrigation canals: technical sessions	T E Brabben & R Wooldridge
OD 119	Performance of Porac Gumain Rivers Irrigation System: Summary Report. In collaboration with NIA.	J A Weller
OD 120	A rapid assessment procedure for identifying environmental and health hazards in & irrigation schemes : Initial evaluation in northern Nigeria	P Bolton, A M A Imevbore P Fraval
OD 121	Socio-economic parameters in designing small irrigation schemes for small scale farmers : The Exchange Case Study	F C Chancellor-Weale
OD 122	Sediment discharge measurements Magat Catchment. Summary Report : 1986-1988	A Dickinson, M B Amphlett & Dr P Bolton
OD 123	Schistosomiasis control measures for small irrigation schemes in Zimbabwe : Results from three years of monitoring at Mushandike Irrigation Scheme	M Chimbari, R J Chitsiko, Dr P Bolton & A J Thomson